

Conformational Dynamics of the Focal Adhesion Targeting Domain Control Specific Functions of Focal Adhesion Kinase in Cells*

Gress Kadaré^{1,2,3}, Nicolas Gervasi^{1,2,3}, Karen Brami-Cherrier^{1,2,3}, Heike Blockus^{1,2,3},
Said el Messari^{1,2,3}, Stefan T. Arold^{4,5}, and Jean-Antoine Girault^{1,2,3#}

¹Inserm, UMR-S 839, F-75005, Paris, France;

²Université Pierre & Marie Curie (UPMC), Sorbonne Universités, F-75005, Paris, France;

³Institut du Fer à Moulin, F-75005, Paris, France;

⁴King Abdullah University of Science and Technology (KAUST), Division of Biological and Environmental Sciences and Engineering, Computational Bioscience Research Center (CBRC), Thuwal, Saudi Arabia.

⁵Centre de Biochimie Structurale, CNRS UMR5048, INSERM U1054, Université de Montpellier I & II, Montpellier, France.

*Running title: *Role of FAT conformational dynamics*

To whom correspondence should be addressed: Jean-Antoine Girault, *Institut du Fer à Moulin*, Inserm UPMC UMR-S 839, 17 rue du Fer à Moulin, 75005 Paris, France, Tel: +33 1 45 87 61 52; Fax +33 1 45 87 61 32; E-mail: jean-antoine.girault@inserm.fr

Key words: protein kinase; tyrosine-protein kinase (tyrosine kinase); focal adhesions; conformational change; protein structure.

Background: FAK is enriched at focal adhesions through its FAT domain, a four-helix bundle.

Results: Mutations that facilitate or prevent opening of the first helix have profound consequences on the biochemical properties of FAK and its function in cells.

Conclusion: The ability of FAT to open and close is essential for FAK function.

Significance: This provides evidence for the functional importance of the conformational dynamics of FAK.

ABSTRACT

Focal adhesion (FA) kinase (FAK) regulates cell survival and motility by transducing signals from membrane receptors. The C-terminal FA targeting (FAT) domain of FAK fulfils multiple functions, including recruitment to FAs through paxillin binding. Phosphorylation of FAT on Tyr⁹²⁵ facilitates FA disassembly and connects to the MAPK pathway through Grb2 association, but requires dissociation of the first helix (H1) of FAT's four-helix bundle. We investigated the importance of H1-opening in cells by comparing the properties of FAK molecules containing wild-type or mutated FAT with impaired or facilitated H1-openings. These mutations did not alter the activation of FAK, but selectively affected its cellular functions, including self-association, Tyr⁹²⁵ phosphorylation, paxillin binding, and FA targeting and turnover. Phosphorylation of Tyr⁸⁶¹, located between the kinase and FAT domains, was also enhanced by the mutation that opened the FAT bundle. Similarly phosphorylation of Ser⁹¹⁰ by ERK in response to bombesin was increased by FAT opening.

Although FAK molecules with the mutation favoring FAT opening were poorly recruited at FAs, they efficiently restored FA turnover and cell shape in FAK-deficient cells. In contrast, the mutation preventing H1 opening markedly impaired FAK function. Our data support the biological importance of conformational dynamics of the FAT domain and its functional interactions with other parts of the molecule.

FAK is a non-receptor tyrosine kinase enriched at focal adhesions (FAs) (1-3). FAK plays a major role in transducing signals downstream from integrins and other membrane receptors (4-6) and it is involved in the control of cell growth, survival, and migration (7,8). Embryonic lethality of the FAK null mutation before mid-gestation underlines its biological importance (9). The overexpression of FAK observed in many tumors correlates with increased tumor invasiveness and metastases, making FAK an attractive therapeutic target (10).

Following integrin engagement by extracellular matrix proteins, FAK is recruited to FAs. The C-terminal focal adhesion targeting (FAT) domain mediates this recruitment by association with paxillin (11,12) through two binding sites for paxillin LD-motifs, formed by helices H1/H4 and H2/H3 on opposite sides of the molecule (13-16). FAT also interacts with talin, which may contribute to recruitment of either partner to FAs (17,18). The molecular basis of the FAK-talin interaction is not known but it seems not to require the structural integrity of FAT (17,19).

Enrichment of FAK at FAs favors its transient dimerization, which triggers trans-autophosphorylation of Tyr³⁹⁷ (20). This is essential

for FAK function, as shown by the embryonic lethality of mutant mice selectively lacking the autophosphorylation site (21). Phosphorylation of Tyr³⁹⁷, which is located in the linker region between the N-terminal FERM (4.1, ezrin, radixin, moesin) (22) and the central kinase domains, allows binding and activation of Src-family kinases (SFKs) (23). Subsequent phosphorylation of Tyr⁹²⁵ by SFKs creates a binding site for the SH2 domain of Grb2, linking FAK to the Ras/extracellular signal-regulated kinase (ERK) pathway (24,25) and facilitating the release of FAK from FAs (26). Tyr⁹²⁵, positioned within H1 of the four-helix bundle, is not accessible for phosphorylation and Grb2 binding (19,27,28). This apparent contradiction suggested that the FAT domain can undergo conformational rearrangement in cells. In support of this hypothesis, H1-swapped dimeric FAT was observed in crystallographic studies, suggesting that H1 has the capacity to dissociate from the rest of the bundle (27). Opening of H1 is likely to result from strain introduced by the P₉₄₄APP motif that connects H1 and H2 (27), because a similar PXP motif triggers domain swapping in p13suc1 (29-31). H1 opening has subsequently been observed in several studies (15,32,33). Conformational strain in this hinge region was experimentally apparent (34,35) and relieved in the open or H1-swapped dimeric conformation of P₉₄₄APP (27,35). The open state would allow Tyr⁹²⁵ phosphorylation and subsequent binding to Grb2. Intriguingly, despite the strain in the H1-H2 hinge region, only 0.1% of FAT Y⁹²⁵E molecules were in the open conformation (33) and only 2.5 % of total FAT were stable, presumably arm-exchanged dimers in size exclusion chromatography analysis (15). The low probability of this transition is consistent with the observation that Tyr⁹²⁵ in the native FAT domain is a much poorer substrate for SFK phosphorylation than are unstructured peptide-mimics of the region around Tyr⁹²⁵ or FAT domains with destabilized cores (27,34,35). Moreover, by severely destabilizing the FAT bundle structure, H1-opening is also predicted to affect other FAT functions, such as paxillin binding and FAK dimerization. Thus, although these data establish that the opening of H1 occurs occasionally *in vitro* and hence might provide a functional switch for FAT, its biological role remains highly questionable.

Here, we investigated the biological importance of FAT dynamics using mutant forms of the isolated FAT domain and of full-length FAK in which the FAT H1-H2 hinge region was modified to increase or decrease its propensity to open (**Fig. 1A**). Our results demonstrate that these mutations have profound consequences on specific FAK functions *in vitro* and *in vivo*. Comparative analysis of the wild-type (wt) and mutant phenotypes strongly supports that the conformational dynamics of FAT are an

essential regulator for the cellular function of wt FAK at FAs.

EXPERIMENTAL PROCEDURES

Antibodies and Reagents.—Rabbit polyclonal antibodies were from the following sources: anti-FAK A17, Santa Cruz Biotechnology (1:2000), anti-phosphoTyr³⁹⁷-FAK (pTyr³⁹⁷-FAK), Biosource (1:2000), anti-pTyr⁹²⁵-FAK, Cell Signaling (1:2000), anti-pTyr⁸⁶¹-FAK or pTyr⁵⁷⁶-FAK, Invitrogen (both 1:1000). Affinity-purified anti-VSV rabbit polyclonal antibodies (1:2000) were a generous gift from M. Arpin (Curie Institute, Paris). A homemade anti-VSV rabbit serum was used for FAK-paxillin immunoprecipitation. Mouse monoclonal antibodies were from the following sources: FAK 4.47 and conformation-specific clone 2A7, Millipore (1:1000), talin, clone 8D4 (1:1000) and anti-VSV, Sigma (1:1000), paxillin, Zymed (1:1000), anti-HA clone 12CA5 and anti-VSV clone P5D4, Roche Molecular Biochemicals (1:500 for immunoprecipitation). All other reagents were from Sigma unless otherwise noted.

DNA Constructs and Mutagenesis.—The N-terminal tagging of full-length rat FAK (AF 020777) by VSV and HA was realized as follows: first a 300-nucleotide (nt) fragment containing a SacII site in the 3' untranslated region of FAK was eliminated by digestion with BamHI-SmaI, filled by T4 DNA polymerase and self-ligated. Then, a new Sac II site was introduced immediately downstream from the FAK ATG start codon, without affecting the primary sequence. Synthetic phosphorylated oligonucleotides corresponding to VSV and HA epitopes flanked by semi-SacII sites were introduced in frame with the FAK sequence in the newly created SacII site, generating the pBKCMV-VSV-FAK and pBKCMV-HA-FAK plasmids. All constructs were verified by DNA sequencing. We used rat FAK^o “standard” isoform, without an additional exon (36).

Mutations in the FAT region of FAK were produced using an XhoI (nt 2950)-SacI (nt 3430) fragment of FAK subcloned in pBlueScript.SK+ (Stratagene) as a template, corresponding pairs of oligonucleotides designed with the desired mutation, and the Quick Change mutagenesis kit from Stratagene. Mutations included replacement of one or several prolines in the hinge between the first two helices of the FAT domain (Pro⁹⁴⁴, Pro⁹⁴⁶, Pro⁹⁴⁷) by glycine residues, producing “relaxed” mutants QGAPP (R-FAK-GP₂), QGAGP (R-FAK-G₂P), and QGAGG (R-FAK-G₃), or deletion of the two residues, producing “tense” mutant ₂P-PP (T-FAK). R-FAK-G₃ was used in most experiments (unless otherwise specified) and is referred to as R-FAK. After validation of every mutation by sequencing, each mutated version of FAT [fragment XhoI (2950)-SacI (3430)] was cloned back to full-length

VSV- or HA-tagged FAK. A recombinant N-terminally His₆-tagged FAK (His₆-FAK) was produced in a baculovirus-based expression system. The rat cDNA FAK sequence was amplified by PCR from pCMV2-FAK^o using a forward primer introducing a BamHI site and a reverse primer bearing a KpnI site and cloned in the similarly digested pFastBac HT B donor plasmid (Invitrogen).

Determination of improved FAT Structure.—FAT₈₉₂₋₁₀₅₂ was produced and crystallized as reported previously (27). Data were collected at the European Synchrotron Radiation Facility, in Grenoble, France, at beamline ID14-2, using a wavelength of 0.97984Å. However, differently from our previous FAT crystal structures, these crystals were cryo-protected in paraffin oil (Hampton Research) and flash-cooled to 100°K. Data integration, molecular replacement and structure refinement were carried out as described (37) (Table 1). Values shown in the Table indicate that the quality of this structure was within the expected range for a crystal structure of this resolution (see Structure Validation section of the deposited PDB file, 3S9O).

GST Fusion Proteins, Pull-downs and in vitro Kinase Assays.—The FAT domain of FAK (rat FAK₈₉₂₋₁₀₅₃) bearing the mutations in the hinge region were generated by PCR amplification from full-length mutated FAK plasmids and cloned through the BamHI site into the pGEX-6P2 expression vector (Novagen). The recombinant proteins were purified on glutathione-Sepharose 4B columns and cleaved when indicated with 3C protease (GE Healthcare) as described (27). For pull-down assays, 5 µg of GST-FAT on the beads were incubated with 1 µg of cleaved FAT. After incubation at 4°C in 10 mM HEPES, pH 7.4, 150 mM NaCl, 3 mM EDTA on a rotator for 2 h, the complexes were washed three times with the same buffer before elution with SDS-PAGE sample buffer at 100°C.

For in vitro phosphorylation assays, active human GST-Src (Sigma) was used at 0.1 µg/ml to phosphorylate 5 µg of GST-FAT (15 min at 30°C) according to the manufacturer's indications. The reaction was stopped by adding SDS-PAGE sample buffer at 100°C. Then, after separation by SDS-PAGE and transfer to nitrocellulose (GE Healthcare), the phosphorylated proteins were detected by immunoblotting with a phospho-specific anti-pTyr₉₂₅ antibody.

In vitro Interactions with Full-length Proteins.—To explore direct binding of mutated FAK proteins, we used recombinant His₆-FAK produced in a baculovirus system. Sf9 cells were cultured in Insect-XPRESS™ Medium (Cambrex Bio Science). Infection was done using a His₆-FAK-recombinant baculovirus. Cells were harvested 48 hr after infection and recombinant proteins were extracted

and affinity-purified under native conditions on a nickel-chelating resin (Ni-resin, ProBond system, Invitrogen) according to the manufacturer's protocol. After purification, His₆-FAK-containing fractions were pooled and dialyzed for 24 h at 4°C against the “native” buffer (50 mM NaH₂PO₄ pH 8, 0.5 M NaCl) and then immobilized on Ni-resin. In the binding assays, transfected cells were lysed in an immune precipitate wash (IPW) buffer (38) and the lysates containing wild-type (wt) or mutated FAK were pre-cleared with Ni-resin for 1 h at 4°C. Pre-cleared lysates (500 µl) were incubated with 1 µg of recombinant His₆-FAK-immobilized on Ni-beads for 2 h at 4°C with constant rocking. Finally, samples were washed three times with the IPW buffer and the bound proteins were eluted by boiling in a Laemmli sample buffer and analyzed by SDS-PAGE followed by immunoblotting with anti-tag antibodies. An unrelated protein, the splicing factor His₆-U2AF protein (a gift from A. Maucuer, *Institut du Fer à Moulin*, Paris) was used in parallel as a specificity control.

Surface Plasmon Resonance.—Binding experiments were performed at 25°C in 0.01 M HEPES buffer at pH 7.4 containing 0.15 M NaCl, 3 mM EDTA and 0.005% Surfactant P20 (GE Healthcare), using a Biacore 3000 Instrument (IFR 83 platform, Paris). GST-FAT was covalently coupled to a CM5 sensor chip (GE Healthcare) via its primary amine groups. The analytes (isolated wt FAT, T-FAT, R-FAT) were injected at various concentrations at a flow rate of 5 µl/min.

Immunoprecipitation.—Forty-eight hours after transfection, COS7 cells were homogenized in modified RIPA buffer (1% Triton X-100 [vol/vol], 5 g/l sodium deoxycholate, 1 g/l SDS, 50 mM Tris [pH 7.4], 150 mM NaCl, 1 mM sodium orthovanadate) and Complete® (Boehringer) protease inhibitors as described (39). For FAK-paxillin-talin co-immunoprecipitations, cells were lysed in FAK-pax buffer (40) (1% [vol/vol] Triton X-100, 150 mM NaCl, 20 mM Tris base, 0.05% [vol/vol] Tween-20, 1 mM NaF, 1 mM Na₃VO₄, supplemented with Complete®. Lysates were pre-cleared by incubation for 1-3 h at 4°C with 100 µl of a mixture (50% each vol/vol) of Sephacryl and protein A- or G- Sepharose beads (GE Healthcare) saturated with 25 g/l BSA. Immunoprecipitation was carried out overnight at 4°C with 40 µl of rabbit anti-VSV serum, or 5 µl of monoclonal anti-VSV or anti-HA antibodies. The beads were washed three times with lysis buffer, resuspended in Laemmli loading buffer, heated at 100°C for 2 min and subjected to SDS-PAGE. Separated proteins were transferred to a nitrocellulose membrane, immunoblotted with the appropriate antibodies and visualized either with horseradish peroxidase-conjugated anti-mouse/anti-rabbit antibodies (1:4000) and the ECL detection system (GE Healthcare) or with IR-Dye 800 CW

donkey anti-mouse/anti-rabbit IgG antibodies (Rockland) and detection by infrared fluorescence with an Odyssey Li-Cor scanner.

Cell Culture and Transfection.—Mouse embryonic FAK *-/-* (*Ptk2 -/-*) fibroblasts (MEFs) (9) were cultured in Dulbecco's modified Eagle's medium (DMEM) supplemented with 10% fetal calf serum (FCS) plus 0.001% (vol/vol) β ME. COS7 cells were cultured in DMEM supplemented with 10% (vol/vol) FCS. MEFs cells were transfected with 1.3 μ g of DNA per 35 mm diameter culture dish with Lipofectamine 2000 (Invitrogen), and COS7 cells were transfected with and 8 μ g DNA per 100-mm-diameter culture dish in the presence of polyethyleneimine as described previously (39). Total DNA quantity was kept constant with empty pcDNA3 plasmid.

Immunofluorescence Microscopy.—Cells were fixed 48 h after transfection in 40 g/l paraformaldehyde (PFA) for 10 min at room temperature (RT), and then permeabilized by incubation for 20 min in PBS containing 0.2% Triton X-100. After saturation with 50 g/l bovine serum albumin (BSA) for 30 min at RT, the coverslips were incubated overnight at 4°C with a 1:500 dilution of monoclonal anti-FAK antibody 4.47, washed in PBS containing 1 g/l BSA and incubated with a 1:1000 dilution of goat anti-mouse antibody conjugated to CY3. The coverslips were washed four times with PBS and mounted in Vectashield (Vector Abcys). The cells were examined at the *Institut du Fer à Moulin* cell imaging facility, with a DM-6000 upright microscope equipped with a SP5 confocal laser scanning device and an argon/krypton laser (Leica Microsystems, Heidelberg, Germany). Circularity was measured with a Fiji plugin: $4\pi \times \text{area}/\text{perimeter}^2$. A value of 1.0 indicates a perfect circle; values between 1.0 and 0.0 indicate an increasingly elongated shape.

Live cell imaging and fluorescence recovery after photobleaching (FRAP) experiments.—The 24 h-transfected cells were plated at low density on 10 μ g/ml fibronectin-coated glass-bottom μ -dishes (35-mm diameter, Biovalley). Twenty-four hours later, the cells were placed in Hank's balanced salt solution (HBSS) at 37°C and imaged with a Leica DMI 4000 inverted microscope (Leica Microsystems) equipped with a confocal spinning disk head (CSU 22; Yokogawa) and a 491 nm laser (MAG Biosystems). The images were acquired with a 63x HCX PL APO (1.4 NA) objective every 5 minutes on an EMCCD camera (QuantEM 512 SC, Photometrics) and analyzed using Metamorph software (Molecular Devices). Up to five different fields were sequentially recorded during each experiment using a Märzhäuser (Wetzlar) automated stage piloted by Metamorph software. Ratios of fluorescence at the FA at each time point to that of the same FA at time 0 were calculated.

In the FRAP experiments, the cells were placed in HBSS medium at 32°C and imaged by a Leica SP5 II upright microscope (Leica Microsystems). The images were acquired with a 40x HCX APO (0.80 NA) water immersion objective and the FRAP experiment performed with the FRAP Wizard software from Leica Microsystems. Five images were taken at low laser intensity (~ 5%) before bleaching at the rate of 1 Hz for measuring the basal fluorescence intensity. Photobleaching was achieved with 100% of the 488 nm laser line with four iterations. Recovery was followed with the same laser power as in the pre-bleached session at the same rate of imaging for 60 s. For each time point, the intensity of the bleached area was normalized to the pre-bleached intensity. Data were corrected for photobleaching due to repeated imaging using parallel measurements in a different region of the cell. FRAP recovery curves and analysis were generated using Igor Pro software (WaveMetrics). To avoid possible artifacts from overexpression, only cells expressing a low but detectable amount of paxillin-GFP were chosen for further analysis.

Statistical analyses.—The data are presented as means \pm SEM for the indicated number of points. Statistical analysis was done with GraphPad Prism 6.0. Comparisons between two sets of means data were done with Student's t test; for three sets or more with one-way ANOVA; and between crossed variables with two-way ANOVA, using Tukey's and Sidak's tests, respectively, for post-hoc comparisons. Values for t, F, and p are indicated in the figure legends.

RESULTS

A mutation designed to open the H1-H2 hinge region increases FAT self-association. We reasoned that if H1 opening of the FAT domain is relevant for selected FAK functions, then these functions would be enhanced by a FAT mutant with enhanced propensity to open H1, and abrogated by a FAT mutant with defective H1 opening, whereas wild-type (wt) FAK would show an intermediate phenotype. Conversely, if the conformational dynamics of FAT were irrelevant for FAK function, then wt FAK would behave like the FAK mutant with abrogated H1 opening. To produce these FAT mutants, we followed an approach previously used to manipulate the domain-opening dynamics of p13suc1 (31). To relieve the strain generated by the prolines in the H1-H2 hinge (P₉₄₄APP), we replaced the hinge prolines with three flexible glycine residues, generating a “relaxed” mutant of FAT (R-FAT, **Fig. 1A**), in which the closed conformation should be stabilized. Conversely, to facilitate FAT opening, we produced a “tense” mutant of FAT (T-FAT) by deleting the two non-proline residues in the proline-rich motif (**Fig. 1A**). Since H1 opening promotes FAT dimerization through H1-exchange *in vitro* (27,35), we performed FAT self-association

experiments to probe H1 release. Wt or mutated FAT was used as bait in pull-down assays with GST-FAT (**Fig. 1B**). Although the 3 forms of FAT were able to bind GST-FAT, T-FAT interacted most strongly (**Fig. 1B, C**). We then studied FAT:FAT interactions by surface plasmon resonance (SPR) with immobilized GST-FAT on the chip (ligand). No binding of GST was detected, whereas all FAT molecules interacted with GST-FAT. As expected, the strongest interaction was observed with T-FAT (**Fig. 1D**). These results from two different approaches show that FAT interacts with itself and that this interaction is increased by a mutation designed to favor FAT bundle opening. At least two mechanisms could account for the FAT:FAT interactions: swapping of helix H1, as observed in some previously published crystals (27) (**Fig. 2A**) and binding of an N-terminal extension of one FAT molecule (residues 895-915) to the paxillin binding site on H1/H4 of another FAT molecule (27) (**Fig. 2B, C**). The improved crystallographic data presented here (**Table 1, Fig 2B, C**) allowed us to ascertain that this second interaction can occur *in cis* (**Fig. 2B**) and *in trans* (**Fig 2C**). However, deletion of residues 895-915 did not prevent the FAT:FAT interaction in pull down or SPR experiments (data not shown), suggesting that the observed dimerization was due to H1-swapping, as expected from the mutant design.

T-FAK mutation promotes interaction between full-length FAK molecules in vitro. To investigate whether FAT mutations could also modify the interaction between full-length FAK molecules, recombinant His₆-FAK bound to Ni-resin was incubated with transfected COS7 cells lysates containing similar levels of VSV-tagged wt FAK, R-FAK or T-FAK (**Fig. 3A**). Retained proteins were detected by immunoblot with anti-VSV antibodies (**Fig. 3B**). Binding of wt FAK and R-FAK to His₆-FAK was similar, whereas binding of T-FAK was consistently stronger (**Fig. 3B, C**). In the same pull-down assay, T-FAK did not bind to an unrelated His₆-tagged-protein on Ni-resin, demonstrating the specificity of the interaction with His₆-FAK (**Fig. 3B, right lane**). Thus, full-length FAK can interact with itself and this interaction is facilitated by the “tense” mutation of the FAT H1-H2 hinge region. It should be emphasized that FAK can self-associate through several mechanisms, including FERM:FERM and FAT:FERM interactions with itself (20).

To distinguish FERM:FAT from FAT:FAT interactions, we carried out pull-down assays using GST alone or fused to FERM or FAT. Equivalent quantities of GST-proteins bound to glutathione-Sepharose beads were used as “bait” and loaded with calibrated amounts of cell lysates from transfected COS7 cells expressing wt or mutant VSV-FAK (**Fig. 3D**). No binding to GST alone was observed (**Fig.**

3D, lanes 1-4). In contrast, FAK:FERM (**Fig. 3D, lanes 6-8, 3E**) and FAK:FAT (**Fig. 3D, lanes 10-12, 3F**) interactions were observed. The T-FAK mutation did not alter the interaction with GST-FERM, whereas it increased the interaction with GST-FAT (**Fig. 3D-F**). Thus, the T-mutation appeared to selectively alter the FAT:FAT interactions, without interfering with the other types of FAK self-association.

Mutations of the H1-H2 hinge alter phosphorylation of Tyr₉₂₅ in solution and in transfected cells. Currently available *in vitro* data suggest that H1 unfolding and dissociation from the FAT core is required for Tyr₉₂₅ phosphorylation by SFKs and subsequent Grb2 SH2 binding (25,27,35). We examined whether mutation of the FAT H1-H2 hinge directly altered phosphorylation of Tyr₉₂₅, using purified FAT domains (892-1052) as substrates for Src *in vitro* (**Fig. 4A, B**). Tyr₉₂₅ was more phosphorylated in T-FAT and slightly less in R-FAT than in wt FAT (**Fig. 4A, B**), providing evidence that the T mutation increased accessibility of Tyr₉₂₅ to SFKs, whereas R mutation decreased it.

We then examined the role of the FAT hinge region in modulating phosphorylation of Tyr₉₂₅ in full-length FAK in transfected COS7 cells. Cells were grown for 48 h in the absence (**Fig. 4C, D**) or presence of 50 μM orthovanadate (**Fig. 4E, F**). Tyr₉₂₅ phosphorylation was slightly decreased in R-FAT and markedly increased in T-FAK (**Fig. 4C-F**). FAT mutants were also co-transfected with B-Fyn to determine their potential to serve as substrates for SFKs in intact cells (**Fig. 4G, H**). T-FAK was markedly phosphorylated by B-Fyn on Tyr₉₂₅, whereas R-FAK phosphorylation was less pronounced (**Fig. 4G, H**). These results confirmed in intact cells the facilitation of Tyr₉₂₅ phosphorylation by H1 opening in T-FAK.

T-FAK mutation increases phosphorylation of FAK on Tyr₈₆₁ but not Tyr₃₉₇ or Tyr₅₇₆ in transfected cells. We then examined whether FAT mutations modified phosphorylation of other key residues in FAK in cells. Using a specific pTyr₃₉₇ antibody, which recognizes the FAK autophosphorylation site (23), we found no difference between mutated and wt FAK in transfected COS7 cells (**Fig. 5A, B**). This indicated that the mutations did not alter Tyr₃₉₇ autophosphorylation or phosphorylation by other kinases. Phosphorylation of Tyr₅₇₆, a residue in the FAK activation loop phosphorylated by SFKs (41), was also unaltered by FAT hinge mutations (**Fig. 5A, C**). In contrast, phosphorylation of Tyr₈₆₁, a residue crucial in oncogenic cell transformation by H-Ras (42), was strongly increased in T-FAK as compared to wt or R-FAK (**Fig. 5A, C**). The lack of change in Tyr₃₉₇ or Tyr₅₇₆ phosphorylation provided strong evidence that increased phosphorylation of Tyr₉₂₅ and Tyr₈₆₁ is a consequence of altered FAT dynamics

and is not mediated by an increased activation of FAK autophosphorylation and/or SFK recruitment.

FAT H1-H2 hinge mutations alter phosphorylation of Ser₉₁₀ in response to bombesin. In addition to tyrosine residues, FAK is phosphorylated on serine residues in response to physiological stimuli (43,44). Ser₉₁₀ is located in the N-terminal extension of FAT that binds back onto the H1/H4 FAT helices in absence of paxillin LD motifs (**Fig. 2B**). A previous study demonstrated that when acting on G protein-coupled receptors, bombesin stimulates FAK Ser₉₁₀ phosphorylation by ERK (45). To investigate the influence of FAT hinge mutations on Ser₉₁₀ phosphorylation, COS7 cells transfected with wt or mutant HA-FAK were serum-deprived for 30 min and incubated with 10 nM bombesin for another 30 min. In response to bombesin, Ser₉₁₀ phosphorylation was stimulated in endogenous and transfected FAK (**Fig. 6A, upper panel**). In T-FAK, basal phosphorylation of Ser₉₁₀ was increased and the effect of bombesin was strongly enhanced as compared to wt FAK (**Fig. 6A, B**). In contrast, bombesin had no effect on Ser₉₁₀ in R-FAK. We verified in the same samples that bombesin also increased ERK phosphorylation and that this effect was unaltered by the presence or absence of wt or mutated FAK (**Fig. 6A, bottom panels**). These results demonstrate that opening of the FAT domain facilitates the phosphorylation of Ser₉₁₀ by ERK in cells.

FAT hinge mutations alter FAK interactions with paxillin but not with talin in cells. The FAT domain contains binding sites for the focal adhesion proteins paxillin and talin, which both participate in the localization of FAK (11,12,17,46). H1 opening and concomitant structural rearrangement of FAT is expected to disrupt the H1/H4 binding site for paxillin LD motifs and to compromise the site on H2/H3 (16,32,33). Talin does not require the structural integrity of the four-helix bundle to bind (14,15,17,19). We investigated the association of mutated FAKs with endogenous paxillin and talin by co-immunoprecipitation. COS7 cells were transfected with wt or mutated VSV-FAK, alone or in combination with B-Fyn. After 48 hours, cells were lysed and the phosphorylation of Tyr₉₂₅ was analyzed by immunoblotting with a phospho-specific antibody (**Fig. 7A, upper panel**). Transfected FAK proteins were immunoprecipitated with an anti-VSV serum and precipitates were immunoblotted with FAK, paxillin or talin antibodies (**Fig. 7A, lower panels**). An increase in paxillin binding was observed for R-FAK as compared to wt FAK (**Fig. 7A, lanes 2, 3, 7B**), in the absence of cotransfection with B-Fyn. In contrast, less paxillin immunoreactivity was associated with T-FAK (**Fig. 7A, lane 4, 7B**). Interestingly, the differences in paxillin binding were amplified by B-Fyn co-expression (**Fig. 7A, lanes 5-7, 7B**). Fyn

strongly enhanced Tyr₉₂₅ phosphorylation in FAK and even more so in T-FAK, whereas R-FAK Tyr₉₂₅ was less phosphorylated (**Fig. 7A, upper panel, lanes 5-7**). The association with paxillin was increased for R-FAK, whereas it was low for T-FAK (**Fig. 7A, lanes 5-7**). Thus, paxillin binding varied in the opposite direction of H1 opening, as expected from the total (H1/H4) and partial (H2/H3) loss of the LD binding sites. Importantly, neither H1-H2 hinge mutations nor cotransfection with Fyn altered the co-immunoprecipitation of talin with FAK (**Fig. 7A, lower panel, 7C**).

FAT hinge mutations alter cell shape and FAK intracellular localization. Given the effects of FAK H1-H2 hinge mutations on paxillin binding, we anticipated that they may also modify FAK targeting in cells. We examined the subcellular localization of these proteins by immunofluorescence in FAK knockout (*Ptk2^{-/-}*) MEFs (9) cotransfected with VSV-tagged wt or mutated FAK and with paxillin-GFP as the FA marker. Twenty-four hours after transfection, cells were fixed and immunostained for FAK (**Fig. 8A**). Cells co-transfected with FAK or T-FAK were generally less round than those transfected only with paxillin-GFP or co-transfected with R-FAK and paxillin-GFP, as shown by superimposing the cell contours (**Fig. 8A, left panel**). Quantification of cell circularity showed that it was lower in cells expressing FAK or T-FAK than in cells not expressing FAK (**Fig. 8B**). R-FAK had no effect on the circularity as compared to untransfected cells (**Fig. 8B**). We then examined the intracellular localization of the various forms of FAK. Wt FAK was, as expected, enriched at FAs, and this enrichment was more pronounced for R-FAK (**Fig. 8C**). In contrast, T-FAK exhibited a diffuse cytoplasmic immunofluorescence with a decreased FA/cytoplasm ratio (**Fig. 8C, D**). In summary, these experiments indicated that although T-FAK was less enriched at FAs than was wt FAK, it had an effect on cell shape, whereas R-FAK was highly enriched at FAs but had no effect on cell shape.

Mutations in the FAT hinge affect focal adhesion turnover. Cell motility depends in part on the ability of FAK to facilitate FA turnover. Disassembly of FAs is correlated with the time residency of several proteins at these sites including FAK (47), paxillin (48), and talin (49). Since the rate constant for dissociation of those proteins from FAs is similar (50,51), we analyzed FA turnover by monitoring paxillin-GFP FRAP in FAK KO MEFs co-expressing wt or mutated VSV-FAK. Although $t_{1/2}$ was not significantly altered (**Fig. 9A, B**), the mobile fraction of paxillin-GFP was increased at FAs in cells expressing wt or T-FAK, whereas R-FAK had no effect (**Fig. 9C**). Similarly, a point mutant of FAK in which Tyr₉₂₅ was replaced by Phe (Y925F) had no effect on paxillin-GFP recovery (**Fig. 9C**). No

change was observed in the cytoplasm away from FAs (Fig. 9D).

To further characterize the effects of FAT mutations on the dynamic properties of FAs, FAK KO MEFs were co-transfected with VSV-FAK and paxillin-GFP and recorded for one hour by time-lapse confocal microscopy (Fig. 9E). Analysis of sequential images showed that cells lacking FAK or expressing R-FAK or Y925F-FAK displayed FAs of similar stability (Fig. 9E, F). In contrast, expression of wt FAK decreased FA stability and this effect was more pronounced with T-FAK (Fig. 9E, F). These results confirmed the consequences of the FAT H1-H2 hinge mutation on FA dynamics and supported the role of FAT opening in FAK function in cell motility.

DISCUSSION

Previous *in vitro* and modeling studies of FAT showed that FAT H1 can spontaneously dissociate from the four-helix bundle (15,27,32-35). This structural rearrangement allows the formation of FAT dimers *in vitro* through H1 swapping (27). In addition, available *in vitro* data suggest that partial detachment of H1 is required for Tyr₉₂₅ phosphorylation by SFKs and subsequent association of pTyr₉₂₅ with Grb2 (27,35). However, H1 opening *in vitro* is a very rare event, occurring only in 2.5% or less of the total FAT population (15). It is therefore unclear if these conformational dynamics of FAT have a biological importance. To address this question, we engineered mutations in the hinge between H1 and H2 of FAT, designed to stabilize (R) or destabilize (T) the FAT four-helix bundle, applying a strategy previously used to modulate domain-opening dynamics in p13suc1 (29-31). We reasoned that any biological effect linked to FAT dynamics would be abrogated in R-FAK and enhanced in T-FAK. Conversely, if FAT dynamics plays only a minor role *in vivo*, comparable to their low occurrence rate *in vitro*, then R-FAK would behave like wt FAK and not produce opposing effects to T-FAK.

In cells, T-FAK displayed increased Tyr₉₂₅ phosphorylation but decreased paxillin binding, whereas opposite effects were observed for R-FAT. These results were in agreement with enhanced opening of the four-helix bundle in T-FAT and lost ability to open in R-FAT. Importantly, the hinge mutations did not impair FAK expression, stability or activation (as indicated by normal levels of phosphorylation on Tyr₃₉₇ and Tyr₅₇₆), showing their specific consequences on FAT functions. The T mutation also increased the ability of FAT to self-associate *in vitro*. Several potential mechanisms could account for FAT:FAT interactions, including H1-swapping and binding of a flexible FAT extension (residues 895-915) to FAT H1-H4 (27) (see Fig. 2). Deletion of residues 895-915 did not

prevent the FAT:FAT interaction, suggesting that interactions of isolated FAT domains result from H1 swapping, although we cannot formally exclude other modes of interaction. We have recently observed that FAK can dimerize through a combination of FERM:FERM and FERM:FAT interactions (20). Interestingly, the present results showed that the T mutation increased the FAT:FAT interaction without interfering with the FAT:FERM interaction.

In spite of the impaired recruitment of T-FAT to FAs, T-FAK preserved its phosphorylation on Tyr₃₉₇, the autophosphorylation site (23), and on Tyr₅₇₆, a residue of the activation loop phosphorylated by SFKs (41). Since autophosphorylation and SFK recruitment are promoted by FAK dimerization (20), it is possible that increased FAT H1 opening in T-FAT favored the H1-swapped dimerization of the mutant protein and thus contributed to the persistence of normal FAK activation in spite of decreased FA recruitment. In cells, formation of H1-swapped wt FAK dimers is likely to be a rare event, although it could conceivably complement the FERM:FERM interaction and replace the FAT:FERM interaction under some circumstances.

In full-length FAK as in purified FAT, Tyr₉₂₅ phosphorylation was increased by the T mutation and tended to be decreased by the R mutation, a contrast enhanced by Fyn co-transfection. Tyr₉₂₅ is an example of a phosphorylation site that has a favorable consensus sequence but a poor conformation for phosphorylation by Src-family kinases (34). Our results indicate that H1 opening allows the helix region surrounding Tyr₉₂₅ to unfold and adopt conformations compatible with kinase interactions, in agreement with a previous report exploring the consequences of the hydrophobic core residue mutations V₉₅₅A/L₉₆₂A (32). Thus, the conformational dynamics of FAT appear to be a biologically important mechanism to control FAK Tyr₉₂₅ phosphorylation and hence FAK interactions with the Ras-MAPK pathway (24,25) as well as the release of FAK from FAs (26).

The T-FAT mutation also enhanced phosphorylation of Tyr₈₆₁, another major substrate residue for SFKs in the FAK C-terminal region (25,41). Tyr₈₆₁ is located in a presumably flexible region of the kinase-FAT linker, more than 50 residues upstream of FAT and about 10 residues upstream of the third Pro-rich motif (PR3). Enhanced Tyr₈₆₁ phosphorylation may be a direct structural consequence of altered conformational FAT dynamics and/or it may result indirectly from increased Tyr₉₂₅ phosphorylation, as the latter has been reported to influence Tyr₈₆₁ phosphorylation (50). FAK is also phosphorylated on several serine residues (44,52) that regulate cell spreading and migration (53). The major such site in the C-terminal

region of FAK is Ser₉₁₀, a substrate of ERK (45). Phosphorylation of Ser₉₁₀ in response to bombesin-induced ERK activation (45) was increased in T-FAK, suggesting that the destabilization of the bundle also increased Ser₉₁₀ accessibility. Ser₉₁₀ is located 15 residues upstream from Tyr₉₂₅, in an N-terminal extension of FAT that can bind back to the FAT surface formed between H1 and H4 (see **Fig. 2B**). This interaction between the N-terminal extension and FAT H1/H4 restricts the accessibility of Ser₉₁₀. Opening of H1 would therefore increase exposure of Ser₉₁₀. Additionally, it is possible that phosphorylation of Tyr₉₂₅ hinders back-binding of the N-terminal extension and thus promotes exposure of Ser₉₁₀. These observations underscore a strong interaction between the FAT domain and the upstream region of the C-terminal moiety of FAK.

Paxillin binding to full-length FAK was impaired by the T mutation and enhanced by the R mutation. These effects were expected because H1 opening and subsequent rearrangement of the FAT structure affect both paxillin binding sites (on H1/H4 and H2/H3) (14,15). Accordingly, R-FAK accumulation at FAs was increased, whereas it was reduced for T-FAK. Interestingly, T-FAK was still found at FAs, although its binding to paxillin was dramatically decreased. This remaining enrichment may result from the residual paxillin binding as well as from paxillin-independent mechanisms (46). Indeed, consistent with previous data showing that integrity of the four-helix bundle was not required for talin binding (17,19), the FAT hinge mutations did not alter the FAK interaction with talin.

FAK is involved in the disassembly of FAs (9) and phosphorylation of Tyr₉₂₅ is implicated in the exclusion of FAK from FAs and promotion of their turnover (26,54). Despite its strongly decreased presence at FAs, T-FAK restored an elongated shape to transfected FAK^{-/-} cells and increased global FA turnover as well as or more efficiently than wt FAK. In contrast, R-FAK was inefficient in spite of its higher enrichment at FAs. The phenotype of R-FAK in these assays was similar to that of Y925F-FAK, previously reported to impair FAK function (50), suggesting that decreased phosphorylation of this residue is an important aspect in R-FAK properties. Remarkably, loss of R-FAK function was very apparent in cells although R-FAK's *in vitro* properties were not very different from those of the wild type, as expected since it stabilized the closed conformation that is likely to be predominant. This contrast clearly underlines the functional importance of FAT dynamics.

Our study provides strong evidence that FAT's structural transitions are physiologically relevant and specifically implicated in key functions of FAK (**Fig. 10** summarizes the working model of FAT's dynamics based on the current study and previous works). It also supports the proposed role of the

P₉₄₄APP motif in the H1-H2 hinge, as the driving force behind H1 opening (27). Interestingly, this motif is conserved among vertebrate FAK, but not in other species (55) or other proteins with FAT-related domains (19). H1 dynamics may therefore be an evolutionarily recent property of FAK. Our results also reveal a functional connection between FAT and the rest of the FAK C-terminal region. An important open question is whether specific factors regulate H1 opening in physiological conditions. Partners of FAK at FAs that could promote its opening are yet to be identified. Other factors, such as local pH changes, could play a role since phosphorylation and conformational dynamics of the FAT domain show some level of sensitivity to changes in pH over a physiological pH range (34). Alternatively, spontaneous FAT opening dynamics may function as a probabilistic switch mechanism, tuned to modulate a sufficiently large FAK subpopulation at sites where FAK is enriched, thus promoting Ras-MAPK signaling and FA disassembly in a time-delayed manner after FAK enrichment (56).

REFERENCES

1. Hanks, S. K., Calalb, M. B., Harper, M. C., and Patel, S. K. (1992) Focal adhesion protein-tyrosine kinase phosphorylated in response to cell attachment to fibronectin. *Proc. Natl. Acad. Sci. USA* **89**, 8487-8491
2. Schaller, M. D., Borgman, C. A., Cobb, B. S., Vines, R. R., Reynolds, A. B., and Parsons, J. T. (1992) pp125^{FAK}, A structurally distinctive protein-tyrosine kinase associated with focal adhesions. *Proc. Natl. Acad. Sci. USA* **89**, 5192-5196
3. Arold, S. T. (2011) How focal adhesion kinase achieves regulation by linking ligand binding, localization and action. *Curr. Opin. Struct. Biol.* **21**, 808-813
4. Parsons, J. T. (2003) Focal adhesion kinase: the first ten years. *J. Cell Sci.* **116**, 1409-1416
5. Schaller, M. D. (2010) Cellular functions of FAK kinases: insight into molecular mechanisms and novel functions. *J. Cell Sci.* **123**, 1007-1013
6. Zachary, I., and Rozengurt, E. (1992) Focal adhesion kinase (p125^{FAK}): A point of convergence in the action of neuropeptides, integrins, and oncogenes. *Cell* **71**, 891-894
7. Mitra, S. K., Hanson, D. A., and Schlaepfer, D. D. (2005) Focal adhesion kinase: in command and control of cell motility. *Nat. Rev. Mol. Cell Biol.* **6**, 56-68
8. Schaller, M. D. (2001) Biochemical signals and biological responses elicited by the

- focal adhesion kinase. *Biochim. Biophys. Acta* **1540**, 1-21.
9. Ilic, D., Furuta, Y., Kanazawa, S., Takeda, N., Sobue, K., Nakatsuji, N., Nomura, S., Fujimoto, J., Okada, M., Yamamoto, T., and Aizawa, S. (1995) Reduced cell motility and enhanced focal adhesion contact formation in cells from FAK-deficient mice. *Nature* **377**, 539-544
 10. Owens, L. V., Xu, L., Craven, R. J., Dent, G. A., Weiner, T. M., Kornberg, L., Liu, E. T., and Cance, W. G. (1995) Overexpression of the focal adhesion kinase (p125^{FAK}) in invasive human tumors. *Cancer Res.* **55**, 2752-2755
 11. Hildebrand, J. D., Schaller, M. D., and Parsons, J. T. (1993) Identification of sequences required for the efficient localization of the focal adhesion kinase, pp125^{FAK}, to cellular focal adhesions. *J. Cell Biol.* **123**, 993-1005
 12. Tachibana, K., Sato, T., D'Avirro, N., and Morimoto, C. (1995) Direct association of pp125^{FAK} with paxillin, the focal adhesion-targeting mechanism of pp125^{FAK}. *J. Exp. Med.* **182**, 1089-1099
 13. Bertolucci, C. M., Guibao, C. D., and Zheng, J. (2005) Structural features of the focal adhesion kinase-paxillin complex give insight into the dynamics of focal adhesion assembly. *Protein Sci.* **14**, 644-652
 14. Gao, G., Prutzman, K. C., King, M. L., Scheswohl, D. M., DeRose, E. F., London, R. E., Schaller, M. D., and Campbell, S. L. (2004) NMR solution structure of the focal adhesion targeting domain of focal adhesion kinase in complex with a paxillin LD peptide: evidence for a two-site binding model. *J. Biol. Chem.* **279**, 8441-8451
 15. Hoellerer, M. K., Noble, M. E., Labesse, G., Campbell, I. D., Werner, J. M., and Arold, S. T. (2003) Molecular recognition of paxillin LD motifs by the focal adhesion targeting domain. *Structure* **11**, 1207-1217
 16. Alam, T., Alazmi, M., Gao, X., and Arold, S. T. (2014) How to find a leucine in a haystack? Structure, ligand recognition and regulation of leucine-aspartic acid (LD) motifs. *Biochem. J.* **460**, 317-329
 17. Chen, H.-C., Appeddu, P. A., Parsons, J. T., Hildebrand, J. D., Schaller, M. D., and Guan, J.-L. (1995) Interaction of focal adhesion kinase with cytoskeletal protein talin. *J. Biol. Chem.* **270**, 16995-16999
 18. Lawson, C., Lim, S. T., Uryu, S., Chen, X. L., Calderwood, D. A., and Schlaepfer, D. D. (2012) FAK promotes recruitment of talin to nascent adhesions to control cell motility. *J. Cell Biol.* **196**, 223-232
 19. Hayashi, I., Vuori, K., and Liddington, R. C. (2002) The focal adhesion targeting (FAT) region of focal adhesion kinase is a four-helix bundle that binds paxillin. *Nat. Struct. Biol.* **9**, 101-106
 20. Bami-Cherrier, K., Gervasi, N., Arsenieva, D., Walkiewicz, K., Bouterin, M. C., Ortega, A., Leonard, P. G., Seantier, B., Gasmi, L., Bouceba, T., Kadare, G., Girault, J. A., and Arold, S. T. (2014) FAK dimerization controls its kinase-dependent functions at focal adhesions. *EMBO J.* **33**, 356-370
 21. Corsi, J. M., Houbron, C., Billuart, P., Brunet, I., Bouvree, K., Eichmann, A., Girault, J. A., and Enslin, H. (2009) Autophosphorylation-independent and -dependent functions of focal adhesion kinase during development. *J. Biol. Chem.* **284**, 34769-34776
 22. Girault, J. A., Labesse, G., Mornon, J. P., and Callebaut, I. (1999) The N-termini of FAK and JAKs contain divergent band 4.1 domains. *Trends Biochem. Sci.* **24**, 54-57
 23. Schaller, M. D., Hildebrand, J. D., Shannon, J. D., Fox, J. W., Vines, R. R., and Parsons, J. T. (1994) Autophosphorylation of the focal adhesion kinase, pp125^{FAK}, directs SH2-dependent binding of pp60^{src}. *Mol. Cell. Biol.* **14**, 1680-1688
 24. Schlaepfer, D. D., Hanks, S. K., Hunter, T., and van der Geer, P. (1994) Integrin-mediated signal transduction linked to Ras pathway by GRB2 binding to focal adhesion kinase. *Nature* **372**, 786-791
 25. Schlaepfer, D. D., and Hunter, T. (1996) Evidence for in vivo phosphorylation of the Grb2 SH2-domain binding site on focal adhesion kinase by Src-family protein-tyrosine kinases. *Mol. Cell. Biol.* **16**, 5623-5633
 26. Katz, B. Z., Romer, L., Miyamoto, S., Volberg, T., Matsumoto, K., Cukierman, E., Geiger, B., and Yamada, K. M. (2003) Targeting membrane-localized focal adhesion kinase to focal adhesions: roles of tyrosine phosphorylation and SRC family kinases. *J. Biol. Chem.* **278**, 29115-29120
 27. Arold, S. T., Hoellerer, M. K., and Noble, M. E. (2002) The structural basis of localization and signaling by the focal adhesion targeting domain. *Structure* **10**, 319-327
 28. Liu, G., Guibao, C. D., and Zheng, J. (2002) Structural insight into the mechanisms of targeting and signaling of focal adhesion kinase. *Mol. Cell. Biol.* **22**, 2751-2760
 29. Bergdoll, M., Remy, M. H., Cagnon, C., Masson, J. M., and Dumas, P. (1997)

- Proline-dependent oligomerization with arm exchange. *Structure* **5**, 391-401
30. Bourne, Y., Arvai, A. S., Bernstein, S. L., Watson, M. H., Reed, S. I., Endicott, J. E., Noble, M. E., Johnson, L. N., and Tainer, J. A. (1995) Crystal structure of the cell cycle-regulatory protein *suc1* reveals a beta-hinge conformational switch. *Proc. Natl. Acad. Sci. USA* **92**, 10232-10236
 31. Rousseau, F., Schymkowitz, J. W., Wilkinson, H. R., and Itzhaki, L. S. (2001) Three-dimensional domain swapping in p13^{suc1} occurs in the unfolded state and is controlled by conserved proline residues. *Proc. Natl. Acad. Sci. USA* **98**, 5596-5601
 32. Dixon, R. D., Chen, Y., Ding, F., Khare, S. D., Prutzman, K. C., Schaller, M. D., Campbell, S. L., and Dokholyan, N. V. (2004) New insights into FAK signaling and localization based on detection of a FAT domain folding intermediate. *Structure* **12**, 2161-2171
 33. Zhou, Z., Feng, H., and Bai, Y. (2006) Detection of a hidden folding intermediate in the focal adhesion target domain: Implications for its function and folding. *Proteins* **65**, 259-265
 34. Cable, J., Prutzman, K., Gunawardena, H. P., Schaller, M. D., Chen, X., and Campbell, S. L. (2012) In vitro phosphorylation of the focal adhesion targeting domain of focal adhesion kinase by Src kinase. *Biochemistry* **51**, 2213-2223
 35. Prutzman, K. C., Gao, G., King, M. L., Iyer, V. V., Mueller, G. A., Schaller, M. D., and Campbell, S. L. (2004) The focal adhesion targeting domain of focal adhesion kinase contains a hinge region that modulates tyrosine 926 phosphorylation. *Structure* **12**, 881-891
 36. Burgaya, F., and Girault, J. A. (1996) Cloning of focal adhesion kinase, pp125FAK, from rat brain reveals multiple transcripts with different patterns of expression. *Mol. Brain Res.* **37**, 63-73
 37. Garron, M. L., Arthos, J., Guichou, J. F., McNally, J., Cicala, C., and Arold, S. T. (2008) Structural basis for the interaction between focal adhesion kinase and CD4. *The Journal of Molecular Biology* **375**, 1320-1328
 38. Dunty, J. M., Gabarra-Niecko, V., King, M. L., Ceccarelli, D. F., Eck, M. J., and Schaller, M. D. (2004) FERM domain interaction promotes FAK signaling. *Mol. Cell. Biol.* **24**, 5353-5368
 39. Kadare, G., Toutant, M., Formstecher, E., Corvol, J. C., Carnaud, M., Bouterin, M. C., and Girault, J. A. (2003) PIAS1-mediated sumoylation of focal adhesion kinase activates its autophosphorylation. *The Journal of Biological Chemistry* **278**, 47434-47440
 40. Ishibe, S., Joly, D., Liu, Z. X., and Cantley, L. G. (2004) Paxillin serves as an ERK-regulated scaffold for coordinating FAK and Rac activation in epithelial morphogenesis. *Mol. Cell* **16**, 257-267
 41. Calalb, M. B., Polte, T. R., and Hanks, S. K. (1995) Tyrosine phosphorylation of focal adhesion kinase at sites in the catalytic domain regulates kinase activity: a role for Src family kinases. *Mol. Cell. Biol.* **15**, 954-963
 42. Lim, Y., Han, I., Jeon, J., Park, H., Bahk, Y. Y., and Oh, E. S. (2004) Phosphorylation of focal adhesion kinase at tyrosine 861 is crucial for Ras transformation of fibroblasts. *The Journal of Biological Chemistry* **279**, 29060-29065
 43. Hunger-Glaser, I., Fan, R. S., Perez-Salazar, E., and Rozengurt, E. (2004) PDGF and FGF induce focal adhesion kinase (FAK) phosphorylation at Ser-910: dissociation from Tyr-397 phosphorylation and requirement for ERK activation. *J. Cell. Physiol.* **200**, 213-222
 44. Ma, A., Richardson, A., Schaefer, E. M., and Parsons, J. T. (2001) Serine phosphorylation of focal adhesion kinase in interphase and mitosis: a possible role in modulating binding to p130(Cas). *Mol. Biol. Cell* **12**, 1-12
 45. Hunger-Glaser, I., Salazar, E. P., Sinnett-Smith, J., and Rozengurt, E. (2003) Bombesin, lysophosphatidic acid, and epidermal growth factor rapidly stimulate focal adhesion kinase phosphorylation at Ser-910: requirement for ERK activation. *J. Biol. Chem.* **278**, 22631-22643
 46. Cooley, M. A., Broome, J. M., Ohngemach, C., Romer, L. H., and Schaller, M. D. (2000) Paxillin binding is not the sole determinant of focal adhesion localization or dominant-negative activity of focal adhesion kinase/focal adhesion kinase-related nonkinase. *Mol. Biol. Cell* **11**, 3247-3263
 47. Hamadi, A., Bouali, M., Dontenwill, M., Stoeckel, H., Takeda, K., and Ronde, P. (2005) Regulation of focal adhesion dynamics and disassembly by phosphorylation of FAK at tyrosine 397. *J. Cell Sci.* **118**, 4415-4425
 48. Schober, M., Raghavan, S., Nikolova, M., Polak, L., Pasolli, H. A., Beggs, H. E., Reichardt, L. F., and Fuchs, E. (2007) Focal adhesion kinase modulates tension signaling to control actin and focal

- adhesion dynamics. *J. Cell Biol.* **176**, 667-680
49. Millon-Fremillon, A., Bouvard, D., Grichine, A., Manet-Dupe, S., Block, M. R., and Albiges-Rizo, C. (2008) Cell adaptive response to extracellular matrix density is controlled by ICAP-1-dependent beta1-integrin affinity. *J. Cell Biol.* **180**, 427-441
50. Deramautd, T. B., Dujardin, D., Hamadi, A., Noulet, F., Kolli, K., De Mey, J., Takeda, K., and Ronde, P. (2011) FAK phosphorylation at Tyr-925 regulates cross-talk between focal adhesion turnover and cell protrusion. *Mol. Biol. Cell* **22**, 964-975
51. Webb, D. J., Donais, K., Whitmore, L. A., Thomas, S. M., Turner, C. E., Parsons, J. T., and Horwitz, A. F. (2004) FAK-Src signalling through paxillin, ERK and MLCK regulates adhesion disassembly. *Nat. Cell Biol.* **6**, 154-161
52. Grigera, P. R., Jeffery, E. D., Martin, K. H., Shabanowitz, J., Hunt, D. F., and Parsons, J. T. (2005) FAK phosphorylation sites mapped by mass spectrometry. *J. Cell Sci.* **118**, 4931-4935
53. Jiang, X., Sinnett-Smith, J., and Rozengurt, E. (2007) Differential FAK phosphorylation at Ser-910, Ser-843 and Tyr-397 induced by angiotensin II, LPA and EGF in intestinal epithelial cells. *Cell. Signal.* **19**, 1000-1010
54. Hamadi, A., Deramautd, T. B., Takeda, K., and Ronde, P. (2010) Hyperphosphorylated FAK Delocalizes from Focal Adhesions to Membrane Ruffles. *J. Oncol.* **2010**, pii: 932803
55. Corsi, J. M., Rouer, E., Girault, J. A., and Enslin, H. (2006) Organization and post-transcriptional processing of focal adhesion kinase gene. *BMC Genomics* **7**, 198
56. Ladbury, J. E., and Arold, S. T. (2012) Noise in cellular signaling pathways: causes and effects. *Trends Biochem. Sci.* **37**, 173-178

FOOTNOTES

CURRENT ADDRESSES

KBC: University of California at Irvine, USA

HB: *Institut de la Vision*, UMR-S 968 Inserm / UPMC / CNRS 7210, 75012 Paris, France

SeM: University of Franche-Comté, UFR Sciences et Techniques, 25030 Besançon, France

ABBREVIATIONS

The abbreviations used are : BSA, bovine serum albumin; DMEM, Dulbecco's modified Eagle's minimal essential medium; ERK, extracellular signal-regulated kinase; FA, focal adhesion; FAK, focal adhesion kinase; FAT, focal adhesion targeting; FERM, four-point-one, ezrin, radixin, moesin; FRAP, fluorescence recovery after photobleaching; GFP, green fluorescent protein; GST, glutathione S-transferase; H1, first helix of the FAT domain; H2, second helix of the FAT domain; HA, hemagglutinin; HBSS, Hank's balanced salt solution; IPW, immune precipitate wash; MEF, mouse embryonic fibroblasts; PBS, phosphate-buffered saline; PR1, proline-rich motif 1; R-FAT/FAK, relaxed FAT/FAK; RIPA: radio-immunoprecipitation assay; RT, room temperature; SDS-PAGE, sodium dodecyl sulfate-polyacrylamide gel electrophoresis; SFK, Src-family kinase; SH2, Src-homology 2; SPR, surface plasmon resonance; T-FAT/FAK, tense FAT/FAK; VSV, vesicular stomatitis virus.

ACKNOWLEDGEMENTS

We thank Dr. Dusko Ilic (Department of Cell and Tissue Biology, UC San Francisco, San Francisco, CA 94143) for the gift of *Ptk2*^{-/-} fibroblasts, Dr. Monique Arpin (Curie Institute, Paris) for providing anti-VSV antibodies and Dr. Alexandre Maucuer for the gift of His₆-U2AF. We acknowledge the European Synchrotron Radiation Facility for provision of synchrotron radiation facilities and we would like to thank the user support team of beamline ID14-2 for assistance with data recording. This work was supported by *Agence Nationale de la Recherche* (ANR-05-2_42589), *Association pour la Recherche sur le Cancer* (ARC, A05/3/3138), *Fondation pour la Recherche Médicale*, European Research Council, Inserm, UPMC and King Abdullah University of Science and Technology (KAUST). HB was an undergraduate funded by the Paris School of Neuroscience (ENP). J.A. Girault's team is affiliated with the ENP and the Bio-Psy laboratory of excellence.

FIGURE LEGENDS

FIGURE 1. Mutations in the H1-H2 hinge of FAT alter its self-association. **A-** Mutations designed to relax (R) or to increase (T) the tension in the H1-H2 FAT hinge region. **B-** Pull-down assays with immobilized GST-FAT or GST and purified FAT domain: wt-FAT (lane 2, 3), R-FAT (lane 4) and T-FAT (lane 5). Input (lane 1): 1 μ g of soluble FAT equivalent to the total amount used in the pull-down assays. Molecular mass markers positions are indicated in kDa. **C-** Quantification of bound FAT in three independent pull-down experiments (means + SEM, a.u., arbitrary units). One-way ANOVA, $F_{2,6} = 37.7$, $p = 0.0004$, Tukey's test ** $p < 0.01$, *** $p < 0.001$, ns, not significant. **D-** Representative SPR sensorgrams showing the binding curves of purified FAT domains to a sensor chip covalently coated with purified GST-FAT. RU: resonance units. Differential response was obtained by subtracting the signal in the blank channel from that in the experimental channel. Estimated Kd: FAT, $23 \pm 8.6 \mu\text{M}$, T-FAT $1.3 \pm 0.8 \mu\text{M}$, R-FAT $24 \pm 5.5 \mu\text{M}$ (mean \pm SEM, $n=3$).

FIGURE 2. Structural analysis of FAT predicts several possible modes of dimerization. **A-** Crystallographic model for the H1-swapped FAT dimer (PDB accession 1K04). One protomer is shown in grey; the other one is color-ramped from the N-terminus (blue) to the C-terminus (red). **B-** Interaction in *cis* between the N-terminal extension (residues 908-915) and FAT H1/H4 observed in the FAT₈₉₂₋₁₀₅₂ crystal structure determined to a resolution of 2.6 \AA for this study (**Table 1**, PDB accession 3S9O, molecule A is shown). The secondary structure representation is color-ramped as in **A**. Side chains of relevant residues are shown. **C-** Crystallographic model for a potential FAT-FAT interaction *via* swapping of the N-terminal extensions (residues 908-915). This arrangement is also taken from PDB accession 3S9O, molecule C and symmetry-related molecule C.

FIGURE 3. T-FAT mutation increases full-length FAK dimerization and interaction with FAT. **A-C** Mutant and wt FAK proteins with N-terminal VSV tags were expressed by transfection in COS7 cells. **A-** Immunoblotting of FAK in 20% of the amount of cell lysates used for each pull-down. Molecular mass markers positions, kDa. **B-** Cell lysates were loaded onto Ni²⁺ beads coated with recombinant His₆-FAK (left lanes) or a His₆-tagged 65-kDa unrelated protein (right lane). After extensive washing, bound proteins were eluted and the presence of VSV-tagged protein was assessed by immunoblotting. Ponceau red staining of the membrane shows equivalent amounts of His₆-FAK bait. **C-** Quantification of the pull-down experiment performed in triplicate (means + SEM, au, arbitrary units). One-way ANOVA, $F_{(2,6)} = 9.8$, $p = 0.013$, Tukey's test, * $p < 0.05$, ns, not significant. In these experiments, full-length FAK interactions are likely to involve FERM:FERM or FAT:FERM interactions, in addition to the FAT:FAT interactions. **D-** COS7 cell lysates containing identical amounts of VSV-tagged mutant or wt FAK proteins were added to beads coated with GST (lanes 1-4), GST-FERM (lanes 5-8), and GST-FAT (lanes 9-12). After washing and elution, bound FAK was visualized by immunoblotting with VSV antibodies. Equivalent quantities of the three different baits used (GST, GST-FERM and GST-FAT) were revealed by immunoblotting with a GST antibody. Input (20% of the lysate amount used in the pull-down) is shown on either side of the VSV blot. **E, F-** Quantification of the amount of VSV-FAK retained by GST-FERM (**B**) and GST-FAT (**C**) in three independent experiments (means + SEM, au, arbitrary units). One-way ANOVA GST-FERM, no significant difference, GST-FAT, $F_{(2,6)} = 43$, $p < 0.001$, Tukey's test, *** $p < 0.001$, ns, not significant. The T mutation in full-length FAK did not modify its binding to GST-FERM but increased its interaction with GST-FAT. (**A, B, D**) Molecular mass markers positions are indicated in kDa.

FIGURE 4. Mutations of the FAT H1-H2 hinge alter phosphorylation of Tyr₉₂₅. **A-** Purified GST-tagged wt FAT domain (lane 1), R-FAT (lane 2, R-FAT), and T-FAT (lane 3) were incubated with Src (0.1 μg/ml) in the presence of ATP for 15 min at 30°C. Immunoblotting was carried out with Tyr₉₂₅ phospho-specific antibody (pY₉₂₅, upper panel) or a FAK C-terminal antibody (FAK, lower panel). GST-FAT position is indicated by an arrowhead. Note that phosphorylation of a breakdown product with a lower molecular weight was also affected in the same direction as full length FAT-GST by the hinge mutations. **B-** Quantification of three experiments for pY₉₂₅ as in **A-**, corrected for the amount of FAK (means + SEM). One-way ANOVA, $F_{(2,6)} = 105$, $p < 0.0001$, Tukey's test * $p < 0.05$, *** $p < 0.001$, **** $p < 0.0001$. **C-** COS7 cells were transfected with wt or mutated VSV-tagged FAK and pY₉₂₅ and FAK were analyzed by immunoblotting. **D-** Quantification of results in **C**. One-way ANOVA, $F_{(2,6)} = 6.43$, $p < 0.05$. **E, F-** Same as in **C, D**, except that cells were treated for 16 h with 50 μM orthovanadate before lysis. One-way ANOVA, $F_{(2,9)} = 7.28$, $p < 0.05$. **G, H-** Same as in **C, D**, except that FAK was cotransfected with B-Fyn. One-way ANOVA, $F_{(2,6)} = 19.9$, $p = 0.002$. **D, F, H-** Tukey's test, * $p < 0.05$, ** $p < 0.01$. (**A, C, E, G**) Molecular mass markers positions are indicated in kDa. (**C, E, G**) the samples were run on the same gel and blot but intervening lanes were deleted as indicated by a vertical line.

FIGURE 5. Mutation of FAT H1-H2 hinge alters phosphorylation of Tyr₈₆₁ but not Tyr₃₉₇ or Tyr₅₇₆. **A-** COS7 cells were transfected with wt FAK, R-FAK or T-FAK. Representative blots show phosphorylation of Tyr₃₉₇, Tyr₅₇₆, and Tyr₈₆₁ using phospho-specific antibodies (pY₃₉₇, pY₅₇₆, and pY₈₆₁, respectively). Levels of FAK protein were assessed with 4.47 monoclonal antibody (FAK). Molecular mass markers positions are indicated in kDa. **B-D** Quantification of three experiments as in **A-** for pY₃₉₇ (**B**), pY₅₇₆ (**C**), and pY₈₆₁ (**D**), corrected for the amount of FAK (means + SEM). Statistical analysis, one-way ANOVA: pY₃₉₇, $F_{(2,6)} = 3.65$, $p = 0.09$; pY₅₇₆, $F_{(2,6)} = 2.82$, $p = 0.14$; pY₈₆₁, $F_{(6,2)} = 48.1$, $p = 0.0002$, Tukey's post-hoc test *** $p < 0.001$, ns, not significant.

FIGURE 6. Effects of the FAT hinge mutation on Ser₉₁₀ phosphorylation. **A-** COS7 cells transfected with HA-tagged wt FAK, R-FAK, or T-FAK were serum-deprived for 30 min and then treated for another 30 min with 10 nM bombesin before cell lysis. Phosphorylation of Ser₉₁₀ and levels of transfected FAK expression were analyzed by immunoblotting with phospho-specific pS₉₁₀ and HA antibodies (upper panels). In parallel, diphospho-44/42 ERK (pERK) and total ERK were monitored with the corresponding antibodies (lower panels). Molecular mass markers positions are indicated in kDa. **B-** Quantification of three experiments for pS₉₁₀ as in **A-**, corrected for the amount of FAK (means + SEM). Two-way ANOVA, interaction; $F_{(2,8)} = 5.96$, $p = 0.026$, treatment, $F_{(1,4)} = 80.9$, $p = 0.0008$, mutation, $F_{(2,8)} = 44.7$, $p < 0.0001$. Sidak's multiple comparisons test, asterisks, +/- bombesin, °, comparisons between FAK constructs, 1 symbol, $p < 0.05$, 2 symbols, $p < 0.01$, 3 symbols $p < 0.001$.

FIGURE 7. Mutations of the FAT H1-H2 hinge alter interaction of FAK with paxillin but not talin. **A-** COS7 cells were transfected with VSV-tagged wt FAK, R-FAK, or T-FAK, without or with B-Fyn cotransfection, as indicated. Cells were lysed 24 h later and FAK immunoprecipitated with anti-VSV antibodies (IP VSV). Phosphorylated Tyr₉₂₅ was determined in total cell lysates (pY₉₂₅, upper panel). Expression of B-Fyn was detected by immunoblotting. Immune precipitates were probed with FAK, paxillin, and talin antibodies as indicated (lower

panels). Mass markers positions are indicated in kDa. **B-** Quantification of the co-immunoprecipitation of paxillin with FAK as in **(A)** expressed as a ratio of paxillin/FAK, a.u., arbitrary units. Statistical analysis, one-way ANOVA: $F_{(5,18)} = 18.09$, $p < 0.0001$, Tukey's post-hoc test, * $p < 0.05$, ** $p < 0.01$, *** $p < 0.001$, **** $p < 0.0001$. **C-** Quantification of the co-immunoprecipitation of talin with FAK as in **(A)** expressed as a ratio of talin/FAK, a.u., arbitrary units. One-way ANOVA: $F_{(5,18)} = 0.35$, $p = 0.87$. **(B, C)** data are means + SEM.

FIGURE 8. Intracellular localization of FAT H1-H2 hinge mutants. A- FAK $-/-$ fibroblasts were co-transfected with paxillin-GFP without (No) or with various VSV-tagged FAK constructs (wt FAK, R-FAK, or T-FAK, as indicated). FAs were visualized by GFP direct fluorescence (Pax-GFP, green) and FAK localization was determined by immunofluorescence with a FAK monoclonal antibody (4.47, Anti-FAK, red). Cell contours were drawn and overlapped (left panels). Scale bars: 10 μm . **B-** Quantification of the circularity of cell contours in **A-**. Statistical analysis: one-way ANOVA, $F_{(3,39)} = 5.18$, $p = 0.004$, Tukey's test vs no FAK, * $p < 0.05$. **C-** FAK $-/-$ cells were transfected with various FAK constructs, as indicated, and immunostained with FAK antibody. A pile of stacked confocal images is shown with color-coded FAK immunofluorescence intensity. WT and R-FAK immunoreactivity was predominantly found at FAs, whereas T-FAK immunoreactivity was very high in the cytoplasm. Scale bars: 10 μm . **D-** Quantification of results in **C-**. One-way ANOVA, $F_{(2,33)} = 11.73$, $p < 0.0001$; Tukey's test, * $p < 0.05$, **** $p < 0.0001$. Data in **B** and **D** are means + SEM.

FIGURE 9. FAT H1-H2 hinge mutations alter FAs turnover. A-D- FAK KO fibroblasts were co-transfected with paxillin-GFP without (-) or with various VSV-tagged FAK constructs (wt FAK, R, T, or Y925F, as indicated). Fluorescence recovery after photobleaching (FRAP) was measured at FAs (**A, C**) and in the cytoplasm (**B, D**). One-way ANOVA: **(A)** $t_{1/2}$ at FAs, $F_{(4,59)} = 0.42$, $p = 0.79$; **(B)** $t_{1/2}$ in cytoplasm, $F_{(4,20)} = 2.84$, $p = 0.051$ FAs; **(C)** recovery at FAs, $F_{(4,66)} = 8.17$, $p < 0.0001$, Tukey's test, * $p < 0.05$, ** $p < 0.01$, **** $p < 0.0001$; **(D)** recovery in cytoplasm, $F_{(4,20)} = 0.86$, $p = 0.50$. **E-** FAK KO cells were co-transfected as in **A** and FA disassembly was analyzed by spinning disk microscopy for 60 min. The images at t_0 (red) and t_{60} (green) were overlapped to show differences. Disassembly appears in red, newly formed FAs in green and stable FAs in yellow. Scale bar: 10 μm . **F-** Percentage of stable FAs determined as in **C** in three independent experiments with four cells per condition. One-way ANOVA, $F_{4,56} = 8.45$, $p < 0.0001$, Newman-Keuls post-hoc test wt FAK or T-FAK vs no FAK, * $p < 0.05$, *** $p < 0.001$; R-FAK or Y925F vs T-FAK, ° $p < 0.05$. Data in **A-D, F** and **G**, are means + SEM.

FIGURE 10. Model for the role of FAT conformational dynamics in FAK. The FAT four-helix bundle exists in closed (**1**) and open (**2**) conformations in a dynamic equilibrium that is strongly shifted towards the closed state. By decreasing or increasing the propensity of the H1-H2 hinge to open, R-FAK and T-FAK mutants favor the closed and open FAT domain conformation, respectively. The scheme depicts the proposed role of these forms in FAK function at FAs. **1-** The closed conformation of FAT has a strong affinity for paxillin LD motifs (two binding sites in FAT) and FAK can be strongly recruited to FAs through this interaction. However, in this configuration, Tyr₉₂₅ is buried in the four-helix bundle. Ser₉₁₀ and Tyr₈₆₁ are also poorly accessible, possibly because of their masking by intramolecular interactions. FAT may also interact with FERM (20) (not shown in the scheme). **2-** Local accumulation of FAK at FAs promotes FAK dimerization through FERM:FERM interactions (20) (only the

FERM domain of the second FAK molecule is drawn in dark grey). Possibly with the help of co-activators, the association between FERM and kinase domains in the dimer is loosened, which promotes autophosphorylation by intermolecular transphosphorylation of Tyr₃₉₇. The SH3 and SH2 domains of SFK bind to a proline-rich motif (PR1) and pTyr₃₉₇, respectively, in the FERM:kinase linker peptide. Either spontaneously (in a stochastic manner) or in response to unknown factors, H1 dissociates from the rest of the bundle. In the open conformation of FAT, the affinity of paxillin for the H1/H4 binding site on FAT is completely lost. Opening of FAT H1 is also expected to alter the stability and disposition of the other three helices, compromising paxillin binding to the H2/H3 site (32,33); Tyr₉₂₅ is exposed and can be phosphorylated by SFKs and then bind Grb2, which activates the ERK pathway. Through unfolding and/or unmasking of the linker region between FAT and the kinase domain, Ser₉₁₀ and Tyr₈₆₁ become exposed and accessible to ERK and SFKs, respectively. Together with the loss of paxillin affinity, phosphorylation of the above sites contributes to detachment of FAK from FAs for degradation or recycling.

Table 1: Crystallographic Data Collection and Refinement Statistics for FAT

Data collection	
	FAT ₈₉₂₋₁₀₅₂
<i>Space group</i>	C222 ₁
<i>Cell dimensions: a, b, c (Å)</i>	89.92, 223.98, 98.01
<i>Resolution (Å)</i>	30.43 – 2.60 (2.67-2.60) ^a
<i>R_{merge} (%)</i> ^b	10.7 (48.7)
<i>I / σI</i>	11.0 (1.4)
<i>Completeness (%)</i>	84.1 (54.0)
<i>Redundancy</i>	3.2 (2.1)
Refinement	
<i>Resolution (Å)</i>	30.43 – 2.6
<i>No. Reflections used</i>	25973
<i>R_{work} / R_{free} (%)</i> ^{c,d}	23.3 / 28.7
<i>Nr. Atoms: Protein / Solvent</i>	3271 / 36
<i>Mean B-factors (Å²):</i> <i>Refinement / Wilson plot</i>	64.3 / 63.0
<i>R.m.s. deviations</i>	
<i>Bond lengths (Å)</i>	0.021
<i>Bond angles (°)</i>	2.008
<i>Ramachandran plot (%)</i> : <i>most favored / outliers</i>	91.6 / 1.2

^a Values in parentheses are for the highest-resolution shell.

^b $R_{\text{merge}} = \frac{\sum_{hkl} \sum_i |I_i(hkl) - \langle I(hkl) \rangle|}{\sum_{hkl} \sum_i I_i(hkl)}$, where $I_i(hkl)$ and $\langle I(hkl) \rangle$ are the observed individual and mean intensities of a reflection with the indices hkl , respectively; \sum_i is the sum over the individual measurements of a reflection with indices hkl ; and \sum_{hkl} is the sum over all reflections.

$$^c R_{\text{work}} = \frac{\sum_h \left| |F_{O_h}| - |F_{C_h}| \right|}{\sum_h |F_{O_h}|}$$

^d All measured reflections were included in the refinement, except the 2.1% (546 reflections) that were used to calculate R_{free} .

Figure 1

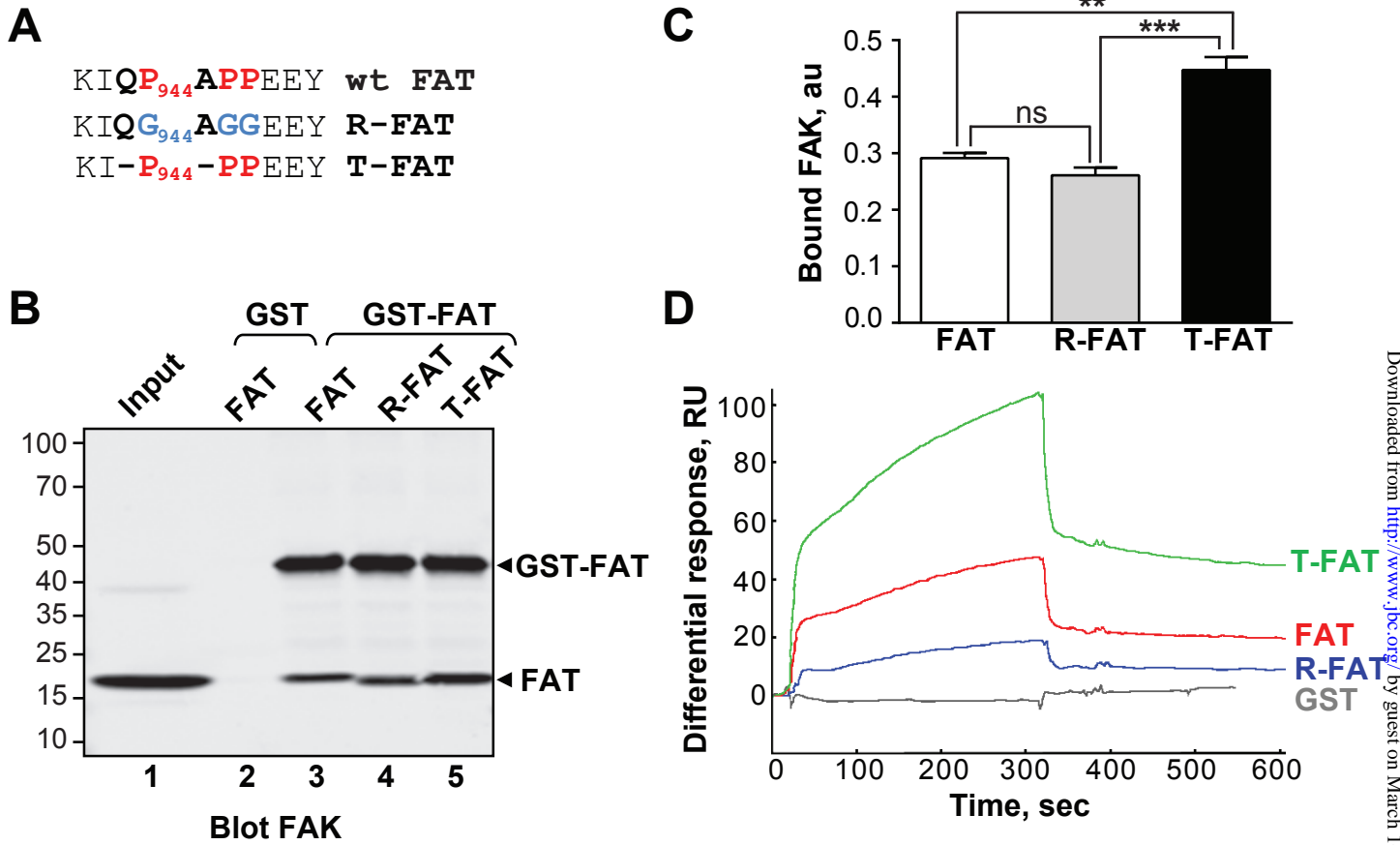


Figure 2

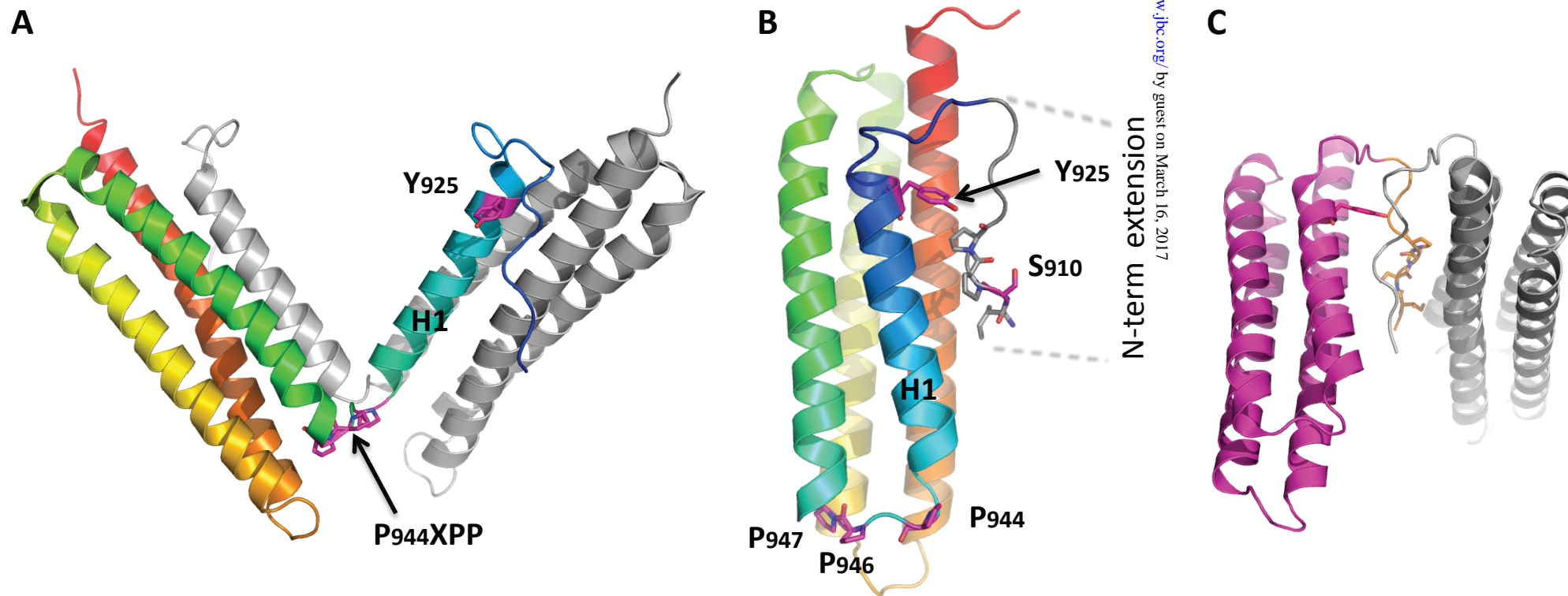


Figure 3

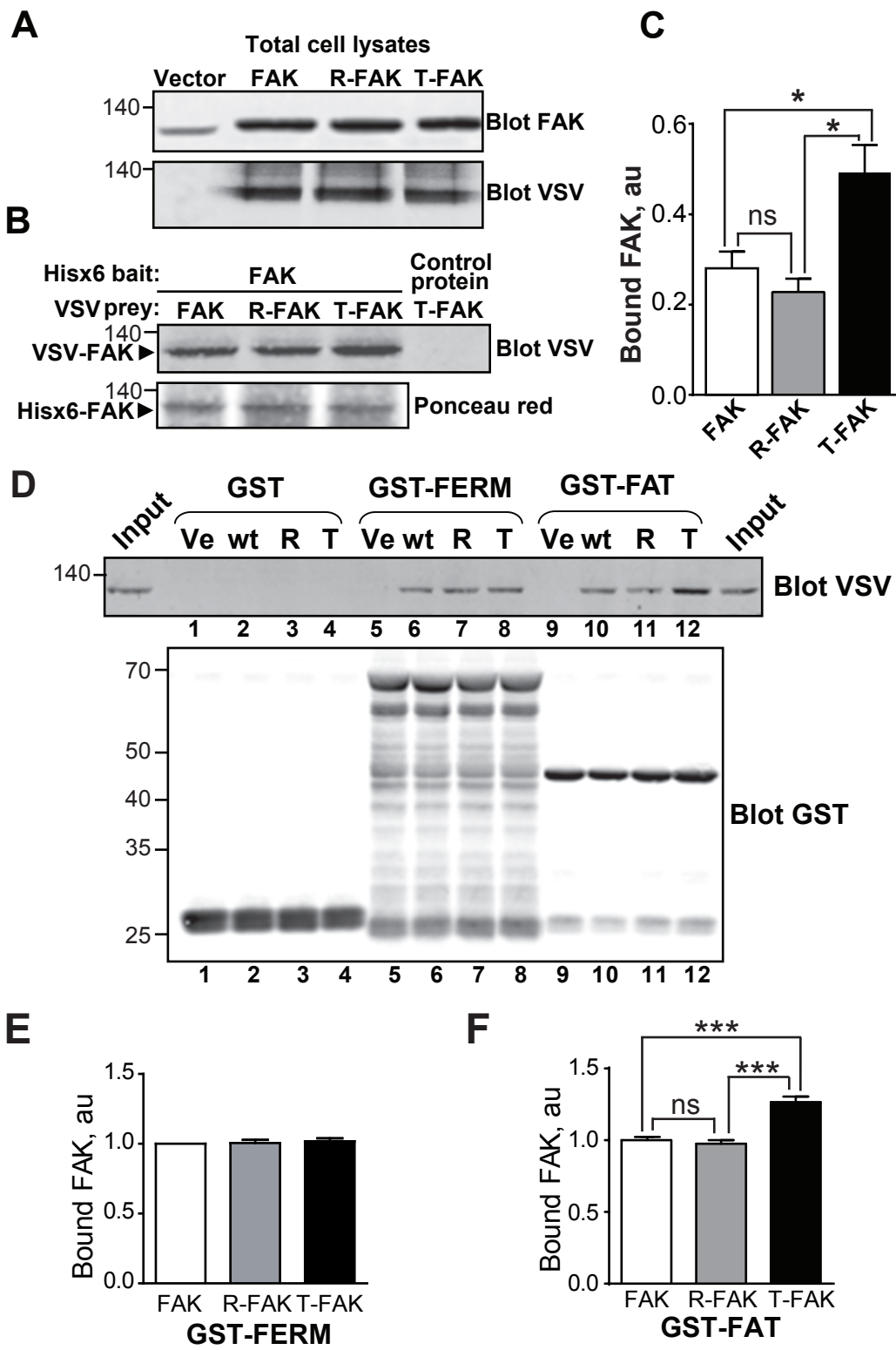


Figure 4

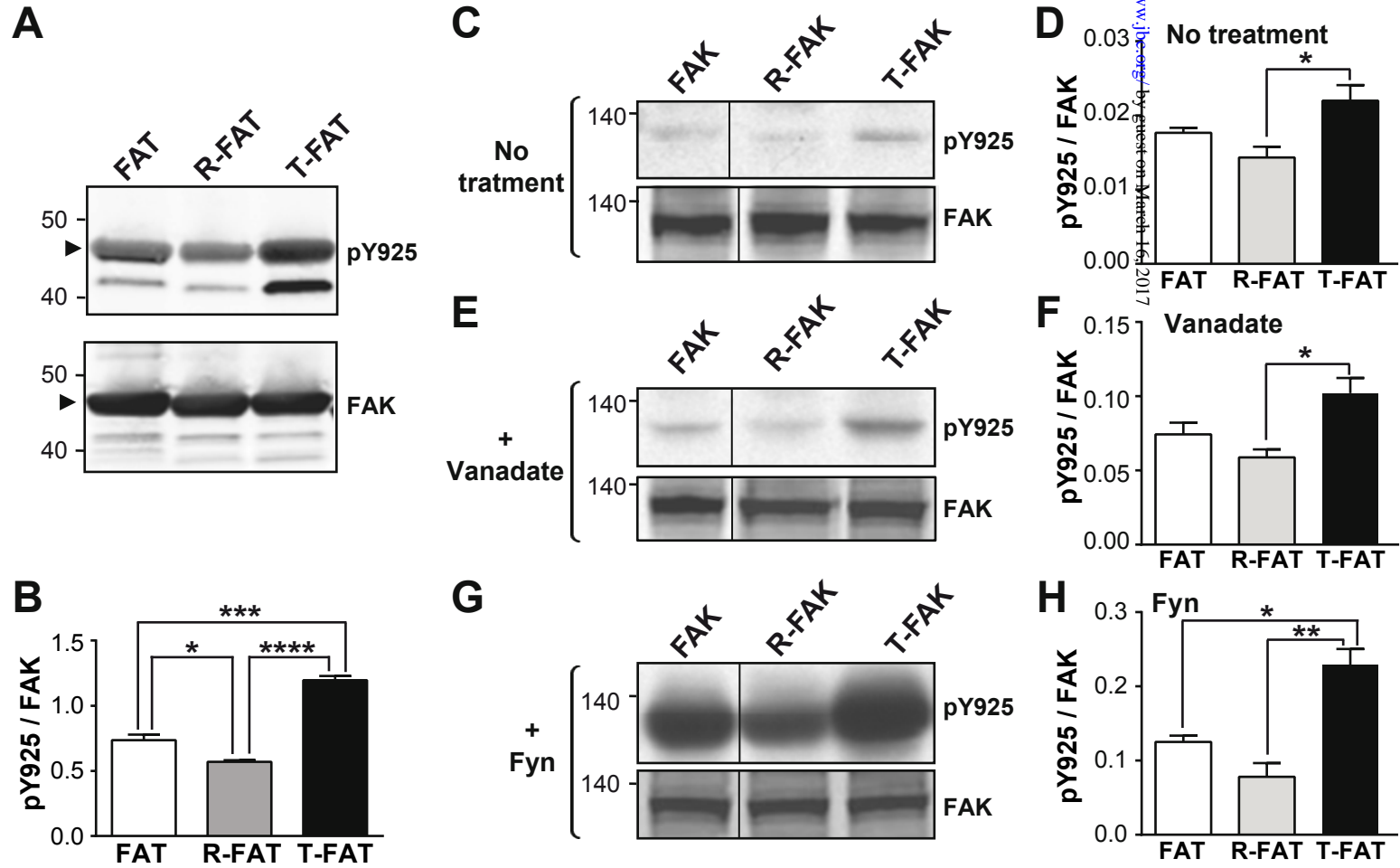


Figure 5

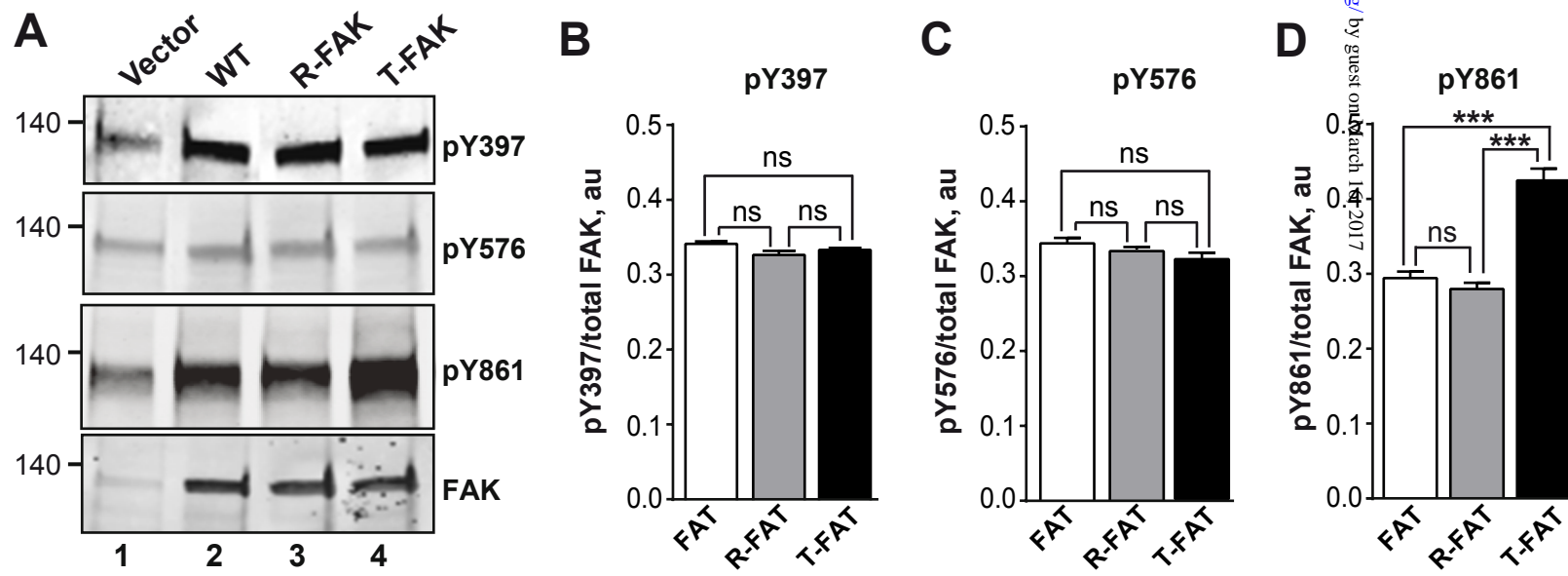


Figure 6

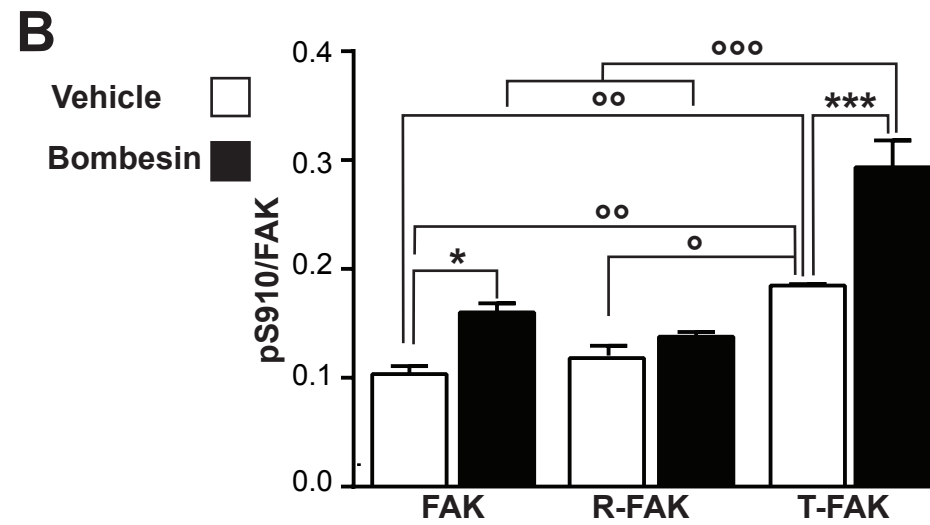
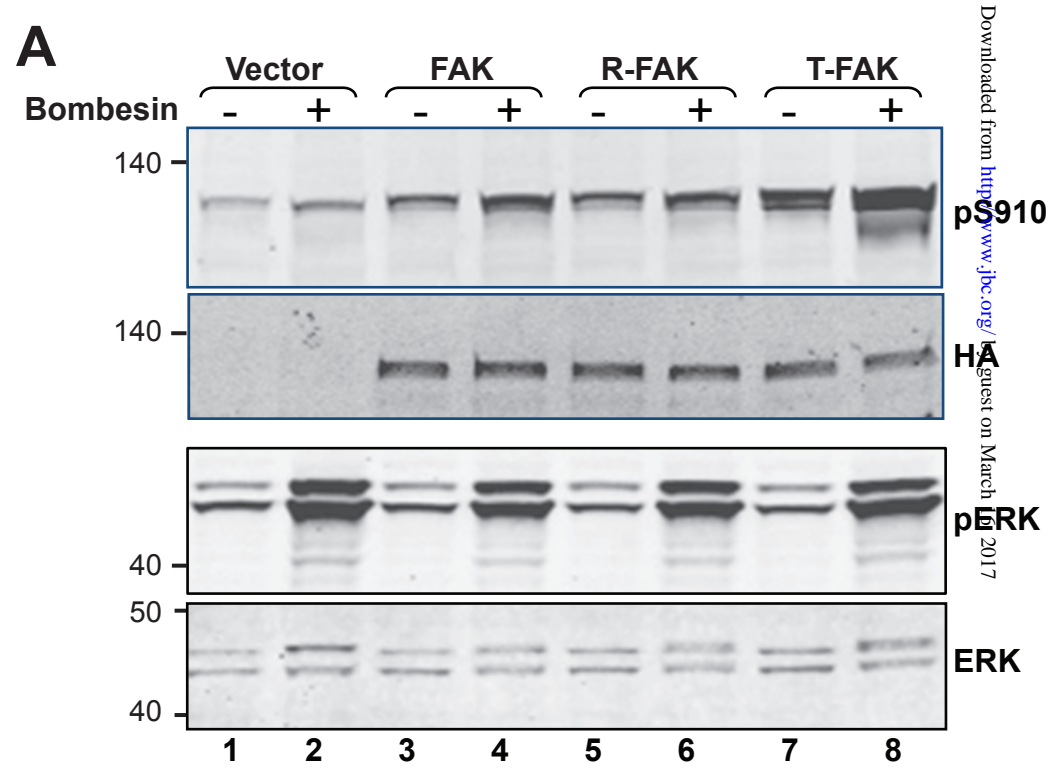


Figure 7

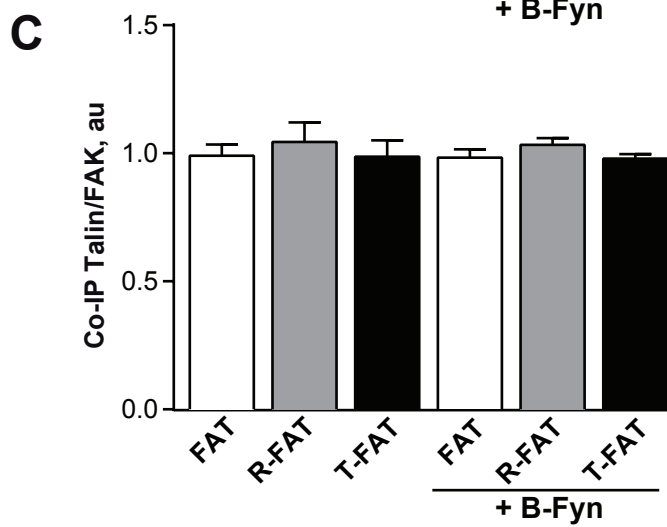
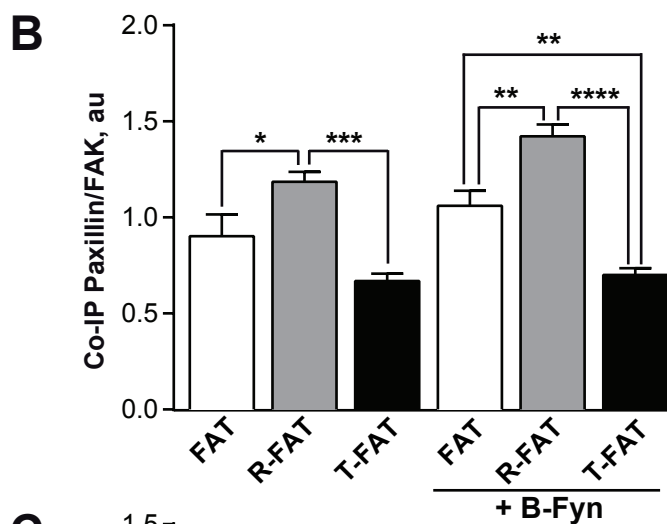
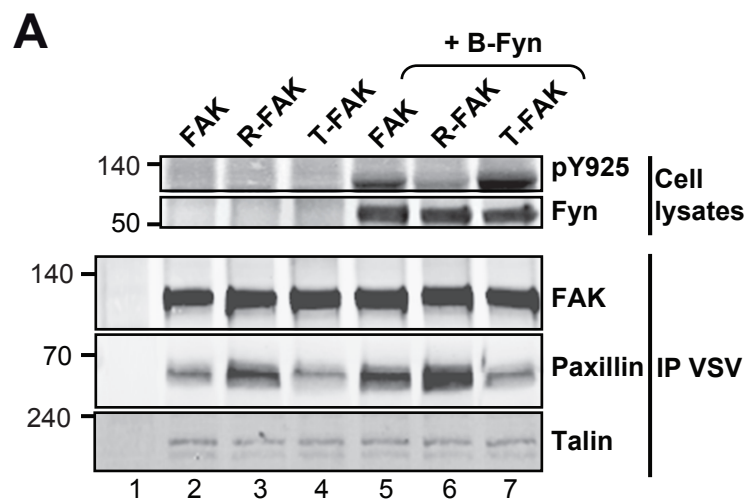


Figure 8

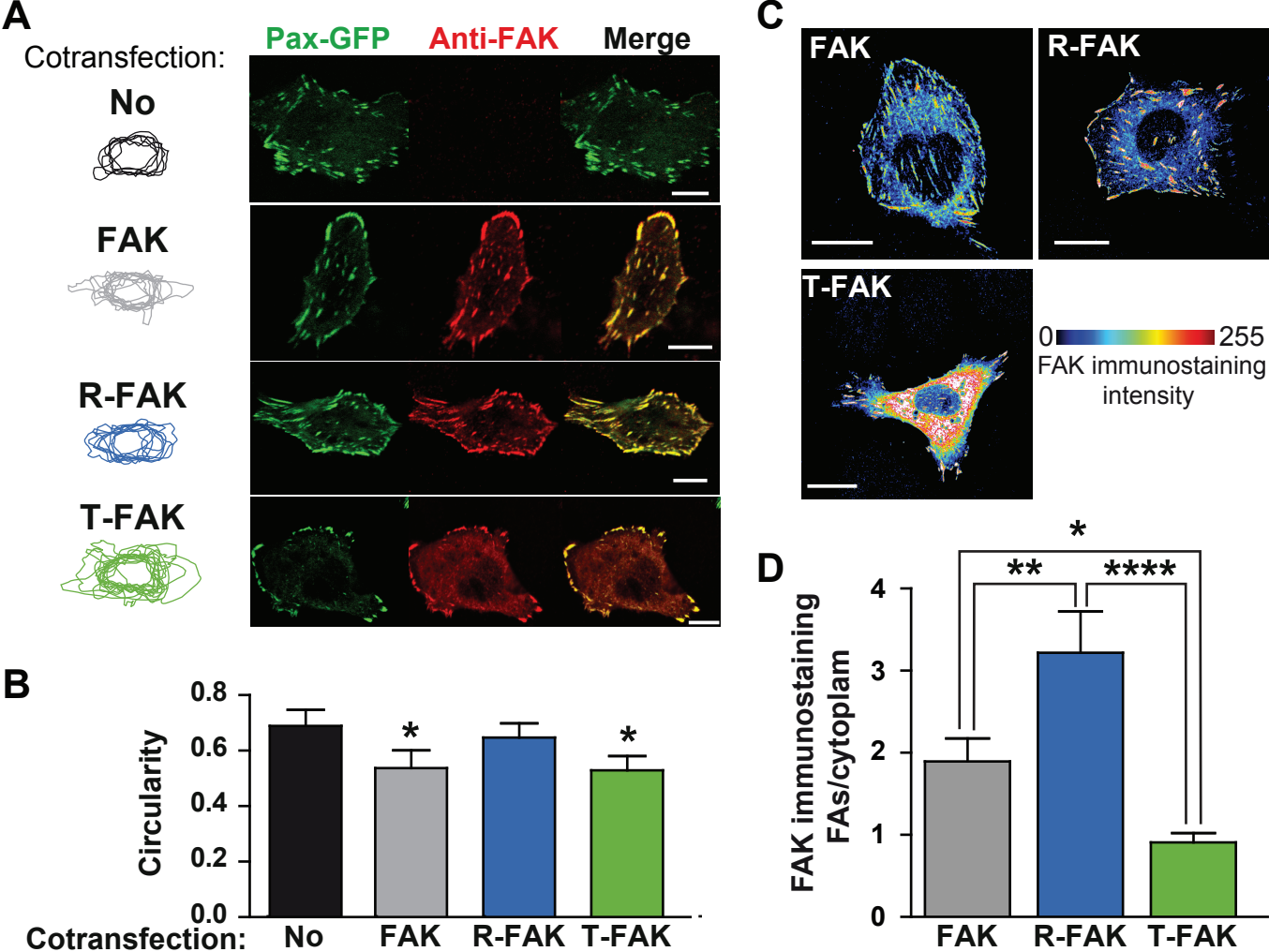


Figure 9

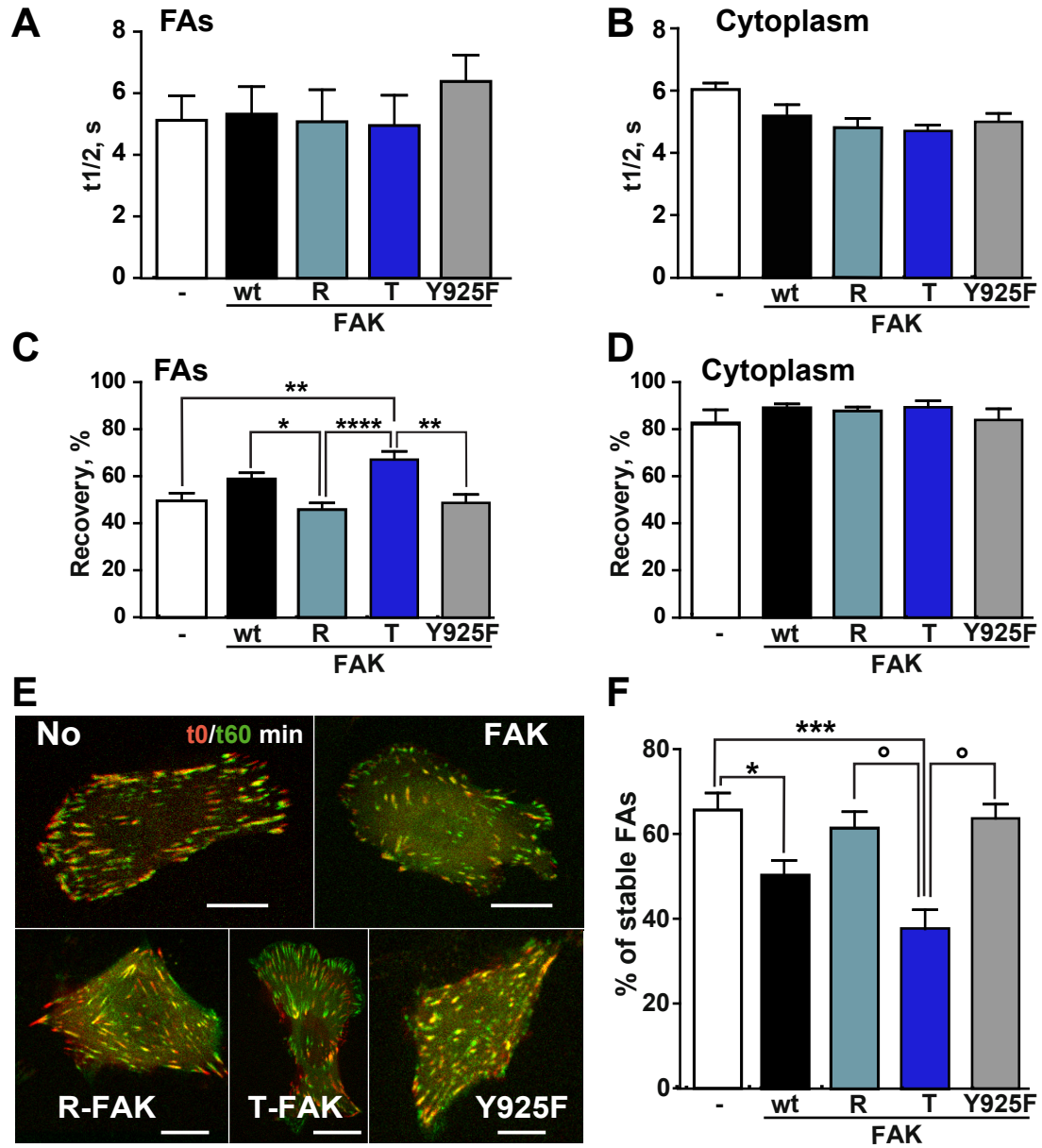


Figure 9

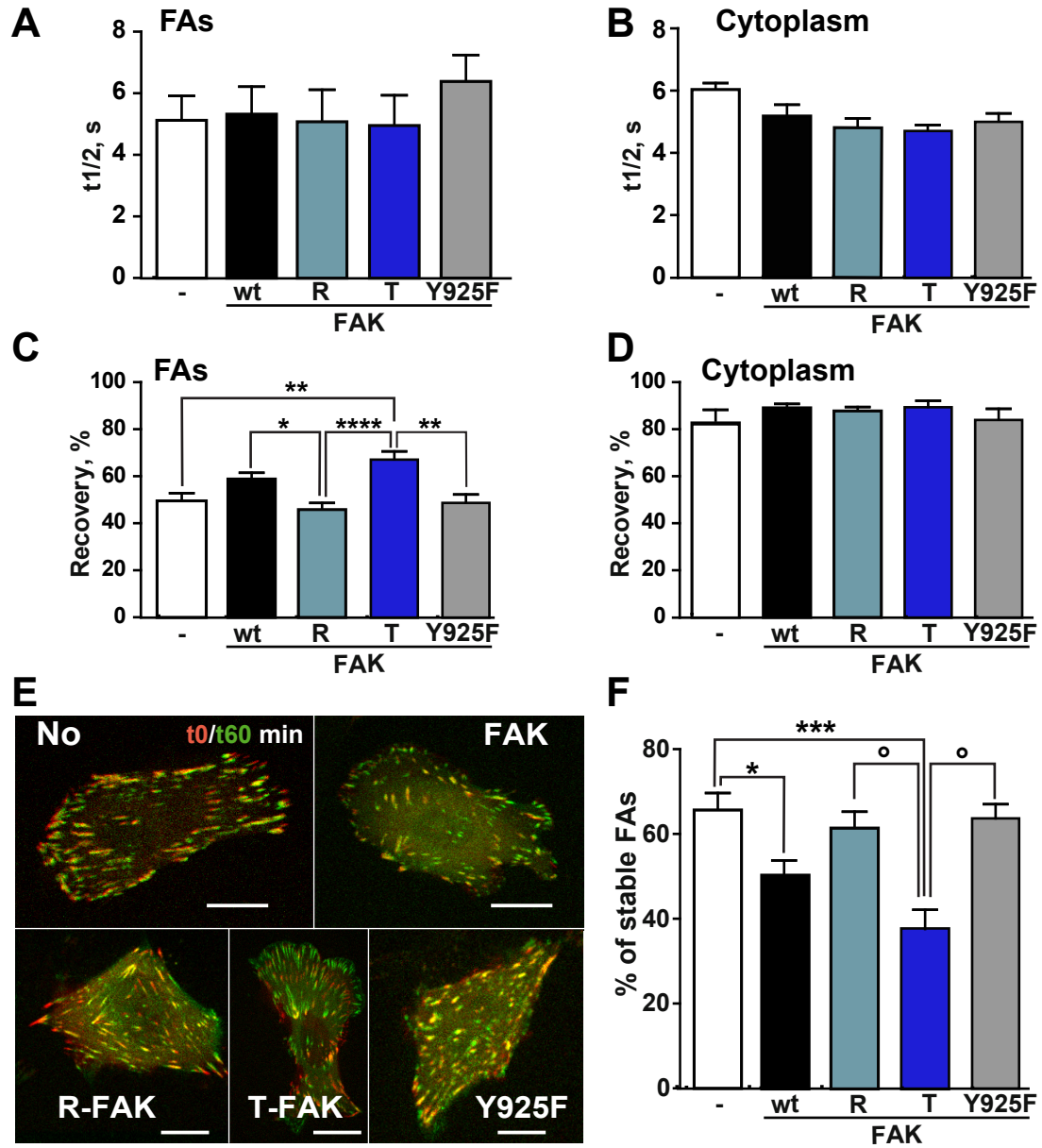
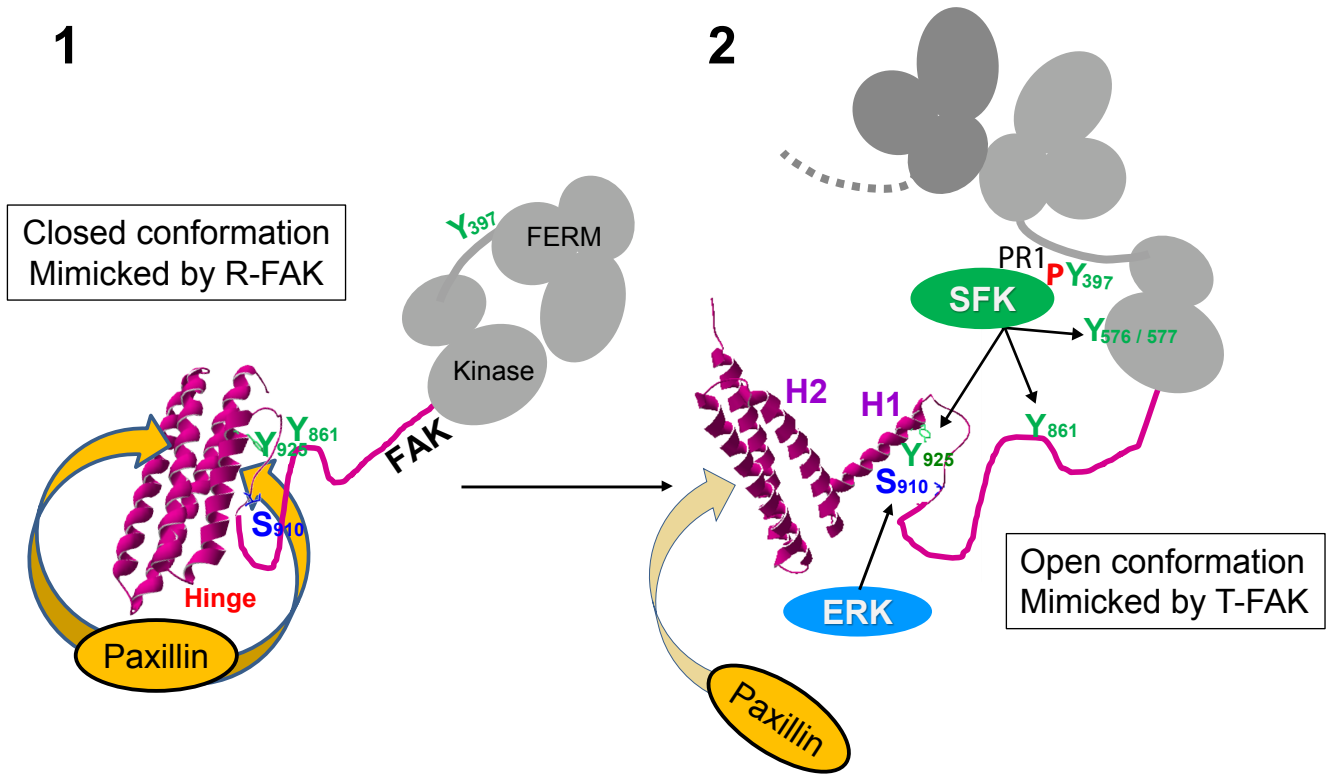


Figure 10



**Conformational Dynamics of the Focal Adhesion Targeting Domain Control
specific functions of focal adhesion kinase in cells**
Gress Kadare, Nicolas Gervasi, Karen Brami-Cherrier, Heike Blockus, Said el Messari,
Stefan T. Arold and Jean-Antoine Girault

J. Biol. Chem. published online November 12, 2014

Access the most updated version of this article at doi: [10.1074/jbc.M114.593632](https://doi.org/10.1074/jbc.M114.593632)

Alerts:

- [When this article is cited](#)
- [When a correction for this article is posted](#)

[Click here](#) to choose from all of JBC's e-mail alerts

This article cites 0 references, 0 of which can be accessed free at
<http://www.jbc.org/content/early/2014/11/12/jbc.M114.593632.full.html#ref-list-1>